



Research paper

Design, synthesis, and biological evaluation of pyrrolopyrimidine derivatives as novel Bruton's tyrosine kinase (BTK) inhibitors



Minjian Yang^{a,1}, Huimin Jiang^{a,1}, Zhuo Yang^a, Xue Liu^a, Hanyu Sun^a, Mengyao Hao^a, Jinping Hu^{b,*}, Xiaoguang Chen^{a,***}, Jing Jin^{a,***}, Xiaojian Wang^{a,****}

^a State Key Laboratory of Bioactive Substances and Functions of Natural Medicines, Institute of Materia Medica, Peking Union Medical College and Chinese Academy of Medical Sciences, Beijing, 100050, China

^b Beijing Key Laboratory of Non-Clinical Drug Metabolism and PK/PD Study, Chinese Academy of Medical Sciences and Peking Union Medical College, Beijing, 100050, China

ARTICLE INFO

Keywords:
BTK inhibitor
Kinase selectivity
B-Cell lymphomas

ABSTRACT

Developing Bruton's tyrosine kinase (BTK) inhibitors has become a significant focus in recent years because BTK inhibition is an effective approach for the treatment of B-cell malignancies. For covalent BTK inhibitors, low oral bioavailability and low kinase selectivity remain unaddressed issues; thus, more diverse inhibitors with both novel structures and selective on target binding profiles are still needed. Here, four key regions where inhibitors bind to BTK were identified by analyzing the existing crystal structures of BTK complexes. Then, a scaffold-based molecular design work flow was established by integrating fragment-growing method, deep learning-based framework XGraphBoost and molecular docking, leading to four compounds that showed potency against BTK. Optimization of compounds 1 and 2 led to the discovery of the potent BTK inhibitor compound 42 by using in vitro potency and pharmacokinetic (PK) studies to prioritize the compounds. Compound 42 exhibited great BTK inhibition activity ($IC_{50} = 0.7 \text{ nM}$) along with high oral absorption. Moreover, 42 demonstrated excellent kinase selectivity, especially over EGFR kinase, and low toxicity. In a TMD8 xenograft model, 42 significantly inhibited tumor growth (TGI = 104%) at a dosage of 50 mg/kg, indicating its potential as a novel therapeutic option for B-cell lymphomas.

1. Introduction

Bruton's tyrosine kinase (BTK) is a member of the Tec family of tyrosine kinases and is expressed in B cells, macrophages, and monocytes but not in T cells, NK cells, and plasma cells [1,2]. In B cells, BTK plays an essential role in B-cell receptor (BCR)-mediated activation and proliferation by regulating the factors downstream of BCR, such as activation of the NF- κ B and MAP kinase pathways [3]. Therefore, dysregulation of BTK generally causes severe leukemias and B-cell-related lymphomas. In addition to its role in BCR signaling, BTK also plays a critical role in Fc receptor (FcR) signaling.

Signaling via Fc γ R-associated receptors promotes BTK-dependent proinflammatory cytokine production by cells such as macrophages

[4]. Consequently, BTK is considered a promising therapeutic target for the treatment of various diseases involving B-cell and/or macrophage activation, such as B-cell malignancies, asthma, rheumatoid arthritis, systemic lupus erythematosus, and multiple sclerosis [5,6].

The first clinically effective covalent BTK inhibitor, ibrutinib (Fig. 1) was approved by FDA in 2013 to treat mantle cell lymphoma (MCL), chronic lymphocytic leukemia (CLL) and Waldenström's macroglobulinemia (WM), and various clinical trials are ongoing for new indications [7–9]. To date, several other BTK inhibitors have been approved (Fig. 1). Acalabrutinib (ACP-196) was approved for the treatment of MCL in 2017 [10]; zanubrutinib (BGB-3111) was given breakthrough therapy designation against MCL and fast track designation for WM by the US FDA in 2019 [11]; tirabrutinib (ONO-4059) was approved for the treatment of recurrent or refractory primary central nervous system

* Corresponding author.

** Corresponding author.

*** Corresponding author.

**** Corresponding author.

E-mail addresses: hujp@imm.ac.cn (J. Hu), chxg@imm.ac.cn (X. Chen), rebeccagold@imm.ac.cn (J. Jin), wangxiaojian@imm.ac.cn (X. Wang).

¹ These authors made equal contributions to this work.

Abbreviations used

BTK	Bruton's tyrosine kinase
BCR	B-cell receptor
PK	pharmacokinetics
FcR	Fc receptors
MCL	mantle cell lymphoma
CLL	chronic lymphocytic leukemia
WM	Waldenström's macroglobulinemia
PCNSL	primary central nervous system lymphoma
SAR	structure–activity relationship.
$t_{1/2}$	half-life.
F	oral bioavailability
DLBCL	diffuse large B-cell lymphoma
MTD	maximum tolerated doses
BID	twicedaily
TGI	tumor growth inhibition
hERG	human ether-a-go-go-related gene
PLC γ 2	phospholipase γ 2
T3P	Propylphosphonic anhydride

lymphoma (PCNSL) in Japan in 2020 [12]; and orelabrutinib received its first approval in China for the treatment of patients with MCL or CLL in December 2020 [13]. In addition to these approved covalent inhibitors, several irreversible inhibitors, such as evobrutinib, spebrutinib and branebrutinib, are in clinical trials. Besides, several noncovalent BTK inhibitors have been reported [14–18]. For irreversible BTK inhibitors, low oral bioavailability and low kinase selectivity remain unaddressed issues that result in the requirement of a high dose in the clinic, which is accompanied adverse effects [19–21]. Thus, more diverse inhibitors with both novel structures and selective on target binding profiles are still needed.

Herein, we aim to discover molecules with improved selectivity and higher oral absorption compared to the currently approved inhibitors.

The initial design was based on analysis of the binding mode of BTK inhibitors to BTK kinase. Then, a scaffold-based molecular design work flow was established by integrating fragment-growing method, deep learning-based framework XGraphBoost and molecular docking, leading to four compounds that showed potency against BTK. We described optimization of compound **1** and **2**, which led to the identification of the potent covalent BTK inhibitor compound **42**. Compound **42** demonstrated excellent kinase selectivity, especially over EGFR kinase, and low toxicity. In a TMD8 cell-derived animal xenograft model, **42** significantly inhibited tumor growth (tumor growth inhibition (TGI) = 104%) at a dosage of 50 mg/kg, indicating its potential as a novel therapeutic option for B-cell lymphomas.

2. Results and discussion

2.1. Design strategy of BTK inhibitors

To identify suitable chemical starting points, this investigation began with the analysis of the eighty-three crystal structures of BTK complexed with both covalent and non-covalent inhibitors, which provided some understanding of key regions for BTK inhibitors to accommodate. As shown on the left side of Fig. 2A, taking the representative covalent inhibitor ibrutinib as an example, covalent inhibitors occupy the hinge region, covalent pocket and back pocket. The hinge region is formed by Glu475 and Met477, which is the conserved region of the ATP binding pocket of the kinase domain. Cys481 is the key residue in the covalent pocket, which provides a Michael donor to form a covalent bond with the inhibitor and is essential for the potency of the molecule. The back pocket is a hydrophobic pocket, containing Phe540 as the key residue. In contrast to covalent inhibitors, noncovalent inhibitors, represented by GDC-0853, mainly occupy the hinge region and H3 pocket. The H3 pocket is formed by Tyr551, Leu542, and Ser543 and has been demonstrated to be essential for obtaining selectivity for BTK versus the other Tec family members [4]. (Fig. S1)

Therefore, there are four key regions for molecule binding to BTK. To obtain a covalent inhibitor, the molecule must occupy the hinge region

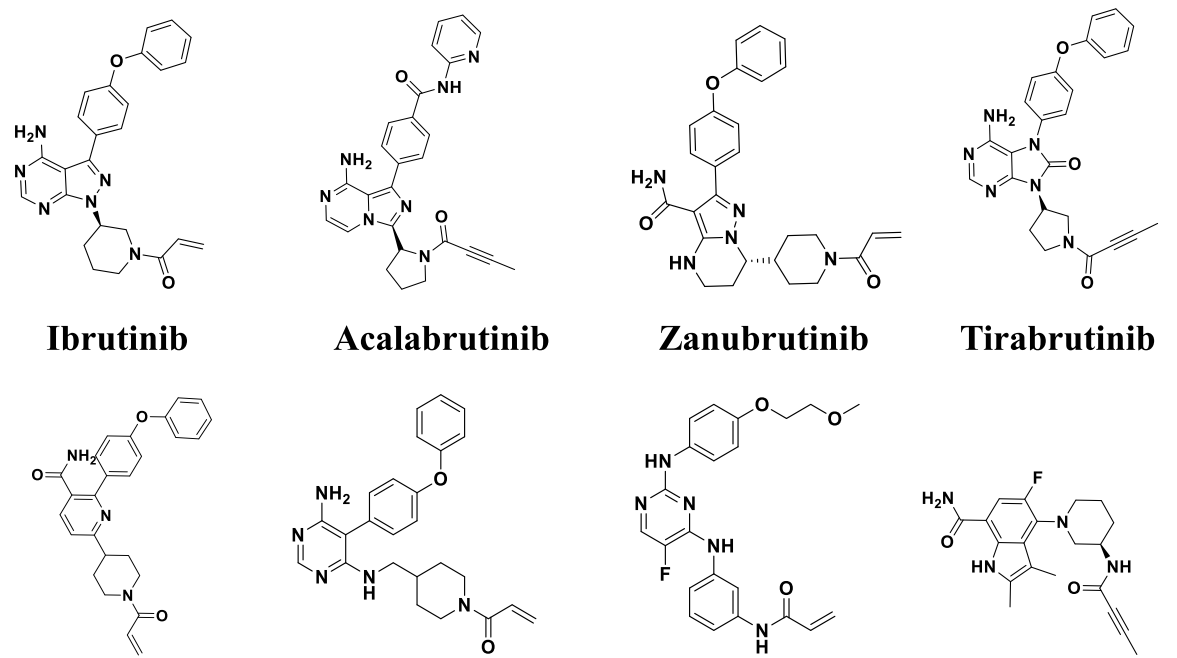


Fig. 1. Structures of approved BTK inhibitors and representative BTK inhibitors in clinical trials.

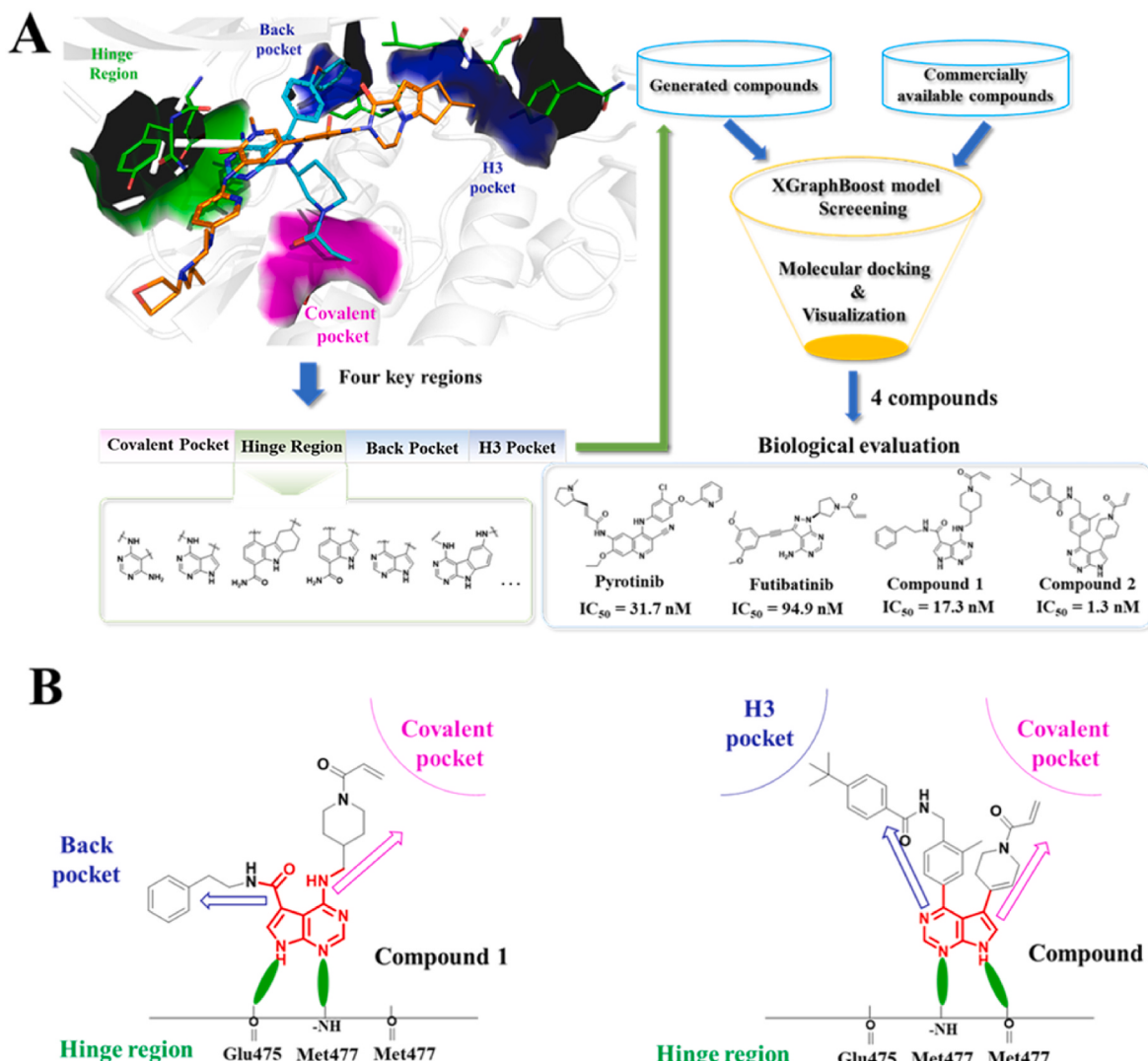


Fig. 2. Characterization of potent BTK inhibitors. (A) Binding mode analysis of ibrutinib (cyan) and GDC-0853 (orange). The key residues are shown in green. Right: Scheme of the fragment-based, XGraphBoost and docking-based design workflow. (B) Predicted binding mode of compounds **1** and **2** with BTK.

and covalent pocket. In addition, the back pocket or H3 pocket should be engaged. Based on the analysis of four key regions, as shown in Fig. 2A, we first obtained a compound library containing 962 compounds based on the preferred fragments of the key regions using a fragment-growing method. Combined with commercially available compound libraries containing 109994 compounds, the structures in the two databases were subjected to the XGraphBoost model to identify the possible BTK inhibitors with predicted active probability greater than 0.5 [22]. 422 compounds were retrieved and were subjected to structure filters. 115 compounds were retained and were docked to the BTK protein to visualize the binding mode of the molecules by Glide in covalent docking mode. Finally, four compounds were selected and subjected to biological evaluation. Among them, pyrotinib and futibatinib were purchased, while compounds **1** and **2** were obtained by synthesis. As shown in Fig. 2A, pyrotinib and futibatinib showed moderate potency against BTK with IC_{50} values of 31.7 and 94.9 nM, respectively. Compounds **1** and **2** showed higher potency against BTK with IC_{50} values of 17.7 and 1.3 nM, respectively. The predicted binding mode and docking score were shown in Fig. S2.

It is worth noting that compounds **1** and **2** bearing the same hinge binder, pyrrolopyrimidine, were predicted to have different binding modes with BTK (Fig. 2B). The pyrrolopyrimidine moiety of compounds **1** and **2** occupies the hinge region. However, the cores in the two

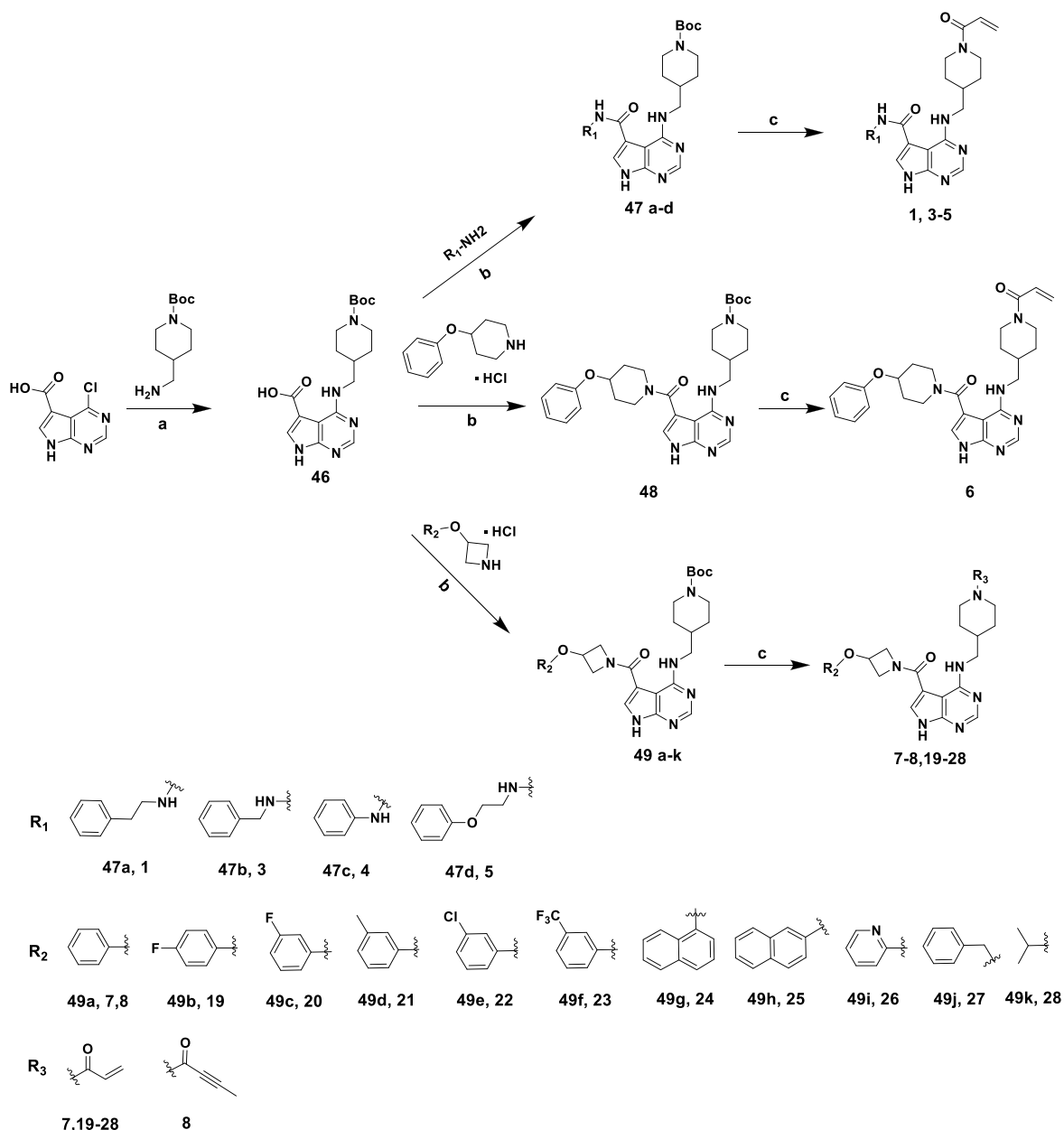
compounds were predicted to take opposite positions. The core of compound **1** formed hydrogen bonds with Glu475 and Met477, and the hydrogen receptor of compound **1** was to the right beside the donor. For the core of compound **2**, only Met477 was involved, and the hydrogen receptor of compound **2** was to the left beside the donor. The cores of compounds **1** and **2** interact with identified hinge region while maintaining the critical vectors and angles required to effectively engage the covalent pocket as covalent BTK inhibitors and orient the phenol group and *tert*-butyl group to the back pocket and H3 pocket, respectively.

Given the high activities and different binding modes derived from the same hinge binder, the two compounds were selected as our hit BTK inhibitors for further structural optimization.

2.2. Chemistry

2.2.1. Synthesis of compound **1** and its derivatives

Compound **1** and its derivatives were prepared as shown in Schemes 1 and 2. Scheme 1 shows the synthesis of compounds **1**, **3–7** and **19–28**. The synthesis started with 4-chloro-7*H*-pyrrolo[2,3-*d*] pyrimidine-5-carboxylic acid and 1-Boc-4-(aminomethyl)piperidine to generate intermediate **46** in 63% yield. Compounds **47a–d**, **48** and **49a–k** were accessed via the T3P- or HATU-mediated amide formation of an aliphatic amine or aniline and the 5-carboxylic acid of **46**. Removal of

**Scheme 1.** Synthesis of compounds 1,3–8, and 19–28^a.

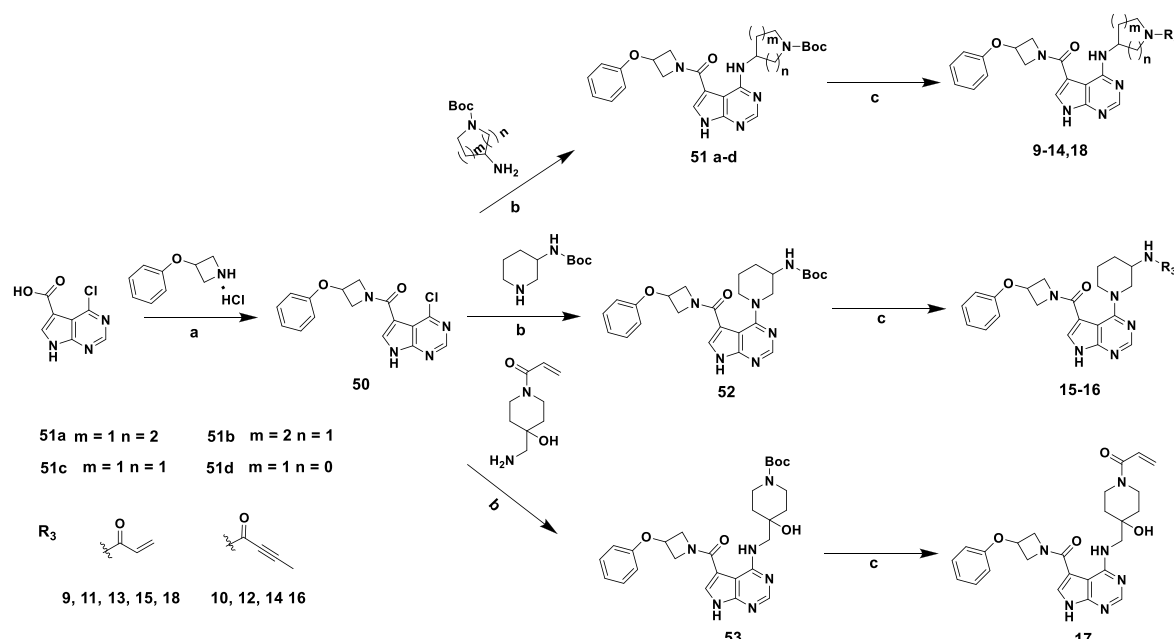
^aReagents and conditions: (a) DIEA, IPA, 80 °C; (b) HATU, DIEA, DMF, rt or T3P, DIEA, THF, rt; (c) (1) TFA, DCM; (2) acryloyl chloride, DIEA, DCM (two steps).

the N-Boc protecting group followed by acylation with acryloyl chloride or butynoyl chloride provided the corresponding compounds 1, 3–8 and 19–28 in 36–52% overall yields. The preparation of compounds 9–18 is illustrated in Scheme 2. The synthesis started from the amide formation of 4-chloro-7*H*-pyrrolo[2,3-*d*]pyrimidine-5-carboxylic acid and 3-phenoxyazetidine hydrochloride, which afforded intermediate 50. Compound 50 was subjected to substitution reactions with aliphatic or alicyclic amines to provide the corresponding intermediates 51a–d, 52 and 53. Removal of the N-Boc protecting group followed by acylation with acryloyl chloride or butynoyl chloride afforded corresponding compounds 9–18 in 37–51% overall yields.

2.2.2. Synthesis of compound 2 and its derivatives

Compound 2 and its derivatives were prepared as shown in Schemes 3–5. Scheme 3 shows the synthesis of compounds 2, 29–33 and 40–43. Intermediates 54a–e were accessed via acylation of (4-bromo-2-R₄-phenyl)methylamine with the appropriate substituted benzoyl chloride.

Borylation of intermediates 54a–e with bis-(pinacolato)diboron in the presence of Pd(dppf)Cl₂ and KOAc gave boronic ester 55a–e. SEM-Cl was used to protect the secondary amino group on 4-chloro-5-iodo-7*H*-pyrrolo[2,3-*d*]pyrimidine to generate SEM-protected compound 56 in 77% yield. The Suzuki reaction of compound 56 and tert-butyl-4-(4,4,5,5-tetramethyl-1,3,2-dioxaborolan-2-yl)-5,6-dihydropyridine-1-(2*H*)-carboxylate gave intermediate 57. Compound 57 was then reacted with boronic esters 55a–e to provide intermediates 58a–e. Removal of the N-Boc protecting group followed by acylation with acryloyl chloride or butynoyl chloride provided corresponding compounds 59a–j in 34–89% overall yields. After deprotection with trifluoroacetic acid, compounds 2, 29–33 and 40–43 were afforded in 69–88% yields. The preparation of compounds 34–39 is outlined in Scheme 4. Reduction of 58a–c was performed with Pd/C and hydrogen to afford intermediates 61a–c. Compounds 61a–c were then subjected to removal of the N-Boc protecting group, acylation with acryloyl chloride or butynoyl chloride and deprotection of the SEM moiety to provide compounds 34–39. As shown

**Scheme 2.** Synthesis of compounds 9–18.^a

^aReagents and conditions: (a) T3P, DIEA, THF, rt, %; (b) DIEA, IPA, 80 °C; (c) (1) TFA, DCM; (2) acryloyl chloride, DIEA, DCM (two steps).

in **Scheme 5**, compounds **44–45** were synthesized in six steps starting with the acylation of (4-bromo-2-fluorophenyl)methylamine with phenyl carbonochloride. Intermediate **62** was then reacted with aniline to provide urea intermediate **63**. Compound **63** was then subjected to borylation followed by a Suzuki reaction with **58** to give intermediate **64**. The Boc group was removed upon treatment with HCl and the compound was acylated with acryloyl chloride or butynoyl chloride. After deprotection with trifluoroacetic acid, compounds **44–45** were afforded in 50% and 61% yields.

2.3. Structure–Activity relationship (SAR) of target compounds

2.3.1. Structural optimization of Compound 1

With the goal of improving potency in the enzymatic assay (<5 nM), various alkane-based linkers between the pyrrolopyrimidine core and the phenyl ring were investigated (**Table 1**). Compared to compound **1** with a phenethylamine group, compound **3** bearing a benzylamine group showed a 2-fold decrease in potency and compound **4** with an aniline group showed a 5-fold decrease in potency. These results showed that reducing the length of the chain linker was detrimental for activity, which indicates that increasing the length may increase activity. Compared to compound **1**, the insertion of an oxygen atom led to an increase in potency (**5**, IC₅₀ of 8.4 nM). Although extending the carbon chain can improve the activity, the IC₅₀ value was still not below 5 nM. We suspect that this may be related to the flexibility of the alkyl chain. To reduce the flexibility of the alkane-based linker, carbon linkers were replaced with piperidine, providing a rigidified exit vector. However, the yielded compound **6** showed decreased potency with an IC₅₀ of 26.2 nM. The docking study showed that compound **6** failed to form interactions with Glu475 and Met477 in the hinge region, which may be due to the steric hindrance of piperidine ring with the surrounding amino acids (**Fig. 3**). To reduce the volume of piperidine ring, a 3-substituted azetidine linker was introduced and was predicted to have the same binding mode as compound **1** (**Fig. 3**). To our delight, switching the piperidine ring to a 3-substituted azetidine linker (**7**) led to a significant improvement in potency with an IC₅₀ of 0.6 nM, which was comparable to that of ibrutinib and higher than that of evobrutinib.

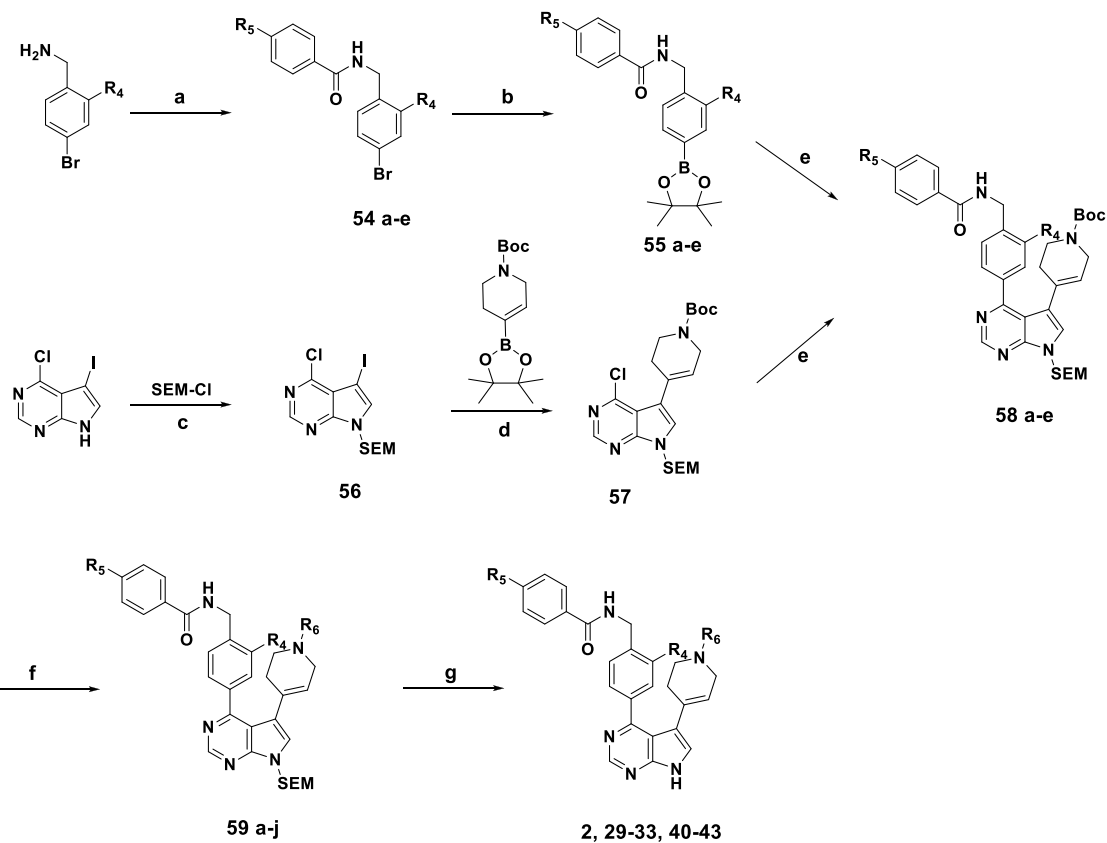
Keeping the 3-substituted azetidine linker unchanged, additional modifications were directed toward the warhead and the linker to the

warhead to further improve the potency against BTK and evaluate the structure–activity relationship (SAR) (**Table 2**). Replacing the acrylamido moiety in **7** with a but-2-ynamido moiety provided compound **8**, which showed an IC₅₀ value of 16.4 nM, which was higher than that of **7**.

(IC₅₀ of 0.6 nM). The position of the warhead in the appropriate location to bind with the BTK Cys481 residue is important for BTK potency as was determined by the N-heterocycle linker. Deletion of the methylene group in compound **7** (compound **9**) significantly reduced the potency, showing an IC₅₀ value of 593.1 nM. In addition, changing the position of the N in the piperidine of compound **9** yielded compound **11**, which retained high potency against BTK with an IC₅₀ value of 1.9 nM. Similarly, compound **13** bearing a pyrrolidine linker showed slightly reduced inhibitory potency for BTK. Continued exploration of the linker moiety showed that attachment of the linker to the hinge binding core via a secondary amine was not tolerated (**15**, IC₅₀ of 5410.2 nM). The replacement of the acrylamido moiety with a but-2-ynamido moiety resulted in a decrease in BTK potency as observed in pairs of modifications (compound **17**).

10 vs. **9**, compound **12** vs. **11**, compound **14** vs. **13**, and compound **16** vs. **15**. Moreover, based on compound **7**, a hydroxyl group was added in compound **17**, which showed similar activity to compound **11**. Finally, replacing the N-heterocycle linker with a nitrogen-linked open chain was not tolerated with respect to BTK inhibition. In conclusion, modifications of warhead and the N-heterocycle linker failed to improve the potency against BTK, and further modifications were still based on compound **7**.

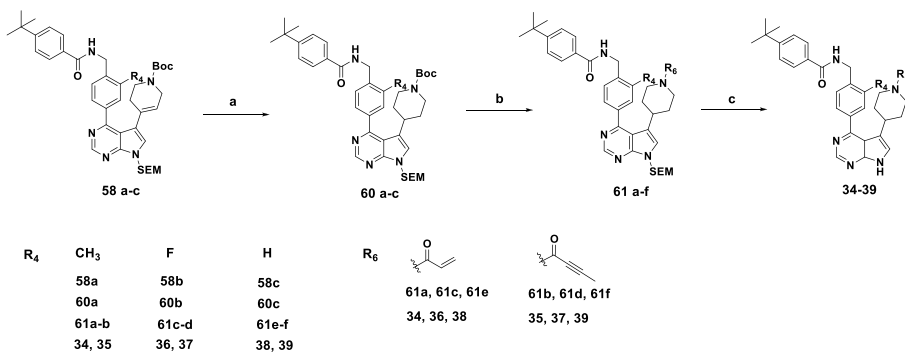
Based on compound **7**, a small series of substituents were introduced to the para position and meta position of the terminal phenyl (**Table 3**). It was found that all the substituents, including 4-F (**19**), 3-F (**20**), 3-CH₃ (**21**), 3-Cl (**22**), and 3-CF₃ (**23**), exhibited comparable effects on BTK inhibition compared to that of compound **7**. Similarly, replacement of the phenyl ring with an α-naphthyl ring and a β-naphthyl ring afforded compound **24** (IC₅₀ of 0.8 nM) and compound **25** (IC₅₀ of 1.4 nM), which exhibited comparable inhibitory potency against BTK compared to compound **7**. Compound **26** bearing a pyridine ring and compound **27** with the insertion of a methene also showed a similar effect on BTK. Finally, phenyl was replaced with isopropyl (**28**), which exhibited more than a 30-fold reduction in biochemical activity. In conclusion, modification of the terminal phenyl moiety successfully yielded a compound



R_4	CH_3	F	H	R_5			R_6		
54a	54b, 54d, 54e		54c	54a-c	54d	54e	59a, 59c,	59b, 59d,	
55a	55b, 55d, 55e		55c	55a-c	55d	55e	59e, 59g,	59f, 59h,	
58a	58b, 58d, 58e		58c	58a-c	58d	58e	59i	59j	
59a-b	59c-d, 59g-j		59e-f	59a-f	59g-h	59i-j	2, 30, 32,	29, 31, 33,	
2, 29	30, 31, 40-43		32, 33	2, 29-33	40, 41	42, 43	40, 42	41, 43	

Scheme 3. Synthesis of compounds 2, 29–33, 40–43^a.

^aReagents and conditions: (a) substituted benzoyl chloride, DIEA, DCM; (b) PinB-BPin, Pd(dppf)Cl₂, KOAc, dioxane; (c) K₂CO₃, DMF, rt; (d) Pd(dppf)Cl₂, K₂CO₃, dioxane/H₂O; (e) Pd(dppf)Cl₂, K₂CO₃, dioxane/H₂O; (f) (1) HCl/EtOH; (2) but-2-ynoyl chloride or acryloyl chloride, DIEA, NaOH, DCM; (g) CF₃COOH, DCM, NaOH (aq).

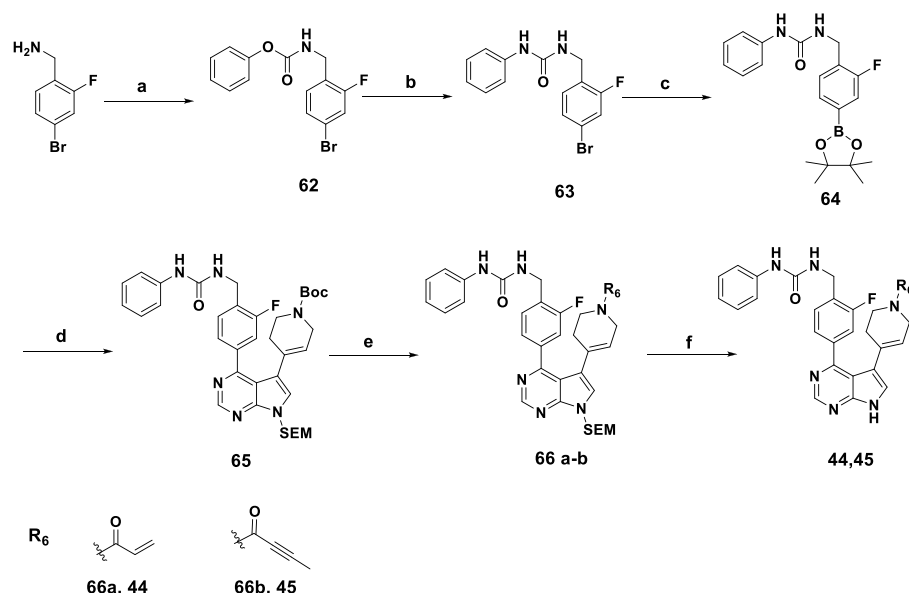
**Scheme 4.** Synthesis of compounds 34-39^a.

^aReagents and conditions: (a) H₂, Pd/C, CH₃OH/EtOAc; (b) (1) HCl/EtOH; (2) but-2-ynoyl chloride or acryloyl chloride, DIEA, DCM; (c) CF₃COOH, DCM, NaOH (aq).

that showed similarly high potency against BTK.

Since the optimized compounds 7, 11, 13, 17, and 19–27 showed high potency against

BTK and the IC₅₀ values were identified to be less than 5 nM, they were selected for an antiproliferative effect study in TMD8 cells. Ibrutinib and evobrutinib were also tested as comparisons. As shown in

**Scheme 5.** Synthesis of compounds 44–45^a.

^aReagents and conditions: (a) phenyl carbonochloride, pyridine, DMF; (b) aniline; (c) PinB-BPin, Pd(dppf)Cl₂, KOAc, dioxane; (d) Pd(dppf)Cl₂, K₂CO₃, dioxane/H₂O; (e) (1) HCl/EtOH; (2) but-2-ynoyl chloride or acryloyl chloride, DIEA, DCM; (f) CF₃COOH, DCM, NaOH (aq).

Table 1
SAR for the Linkers Between the Pyrrolopyrimidine Core and the Phenyl

Compd.	R ₁	BTK IC ₅₀ (nM)
1		17.3
3		52.3
4		98.7
5		8.4
6		26.2
7		0.6
Ibrutinib	—	0.2
Evobrutinib	—	1.83

^a Number of determinations = 1.**Table 4**, compounds 7 and 19–27 showed high potency in TMD8 cells, with IC₅₀ values below 100 nM. Among them, compound 20 exhibited the highest potency with an IC₅₀ of 9.2 nM, which was comparable to that of ibrutinib. In addition, compounds 7 and 20–27 showed higher potency than evobrutinib (IC₅₀ of 56.2 nM).

Inspired by the excellent in vitro potency, we then performed PK parameter testing of the compounds with the aim of finding a compound with an acceptable preclinical PK profile. Both 20 and 22 were selected for the PK study in mice following intravenous

-us (2 mg/kg) and oral (10 mg/kg) administration. Unfortunately, the study on 20 and 22 showed low oral bioavailability values of 2.58% and 1.82%, respectively (Table 5). On the one hand, the low bioavailability could be attributed to the instability azetidine linker might be unstable and prone to ring opening in the gastric fluid environment [17]. However, the high activities of this series of compounds mainly come from the introduction of the 3-substituted azetidine linker. Therefore, it was difficult to further optimize compound 1 to obtain a compound that showed drug candidacy for further profiling, and we had to turn our attention to the optimization of compound 2.

Compared with compound 1, compound 2 showed higher activity with an IC₅₀ of 1.34 nM. Instead of using a 3-substituted azetidine linker to connect the hinge binder and terminal phenyl, a phenyl group, which is a more stable linker, was employed as the linker between the pyrrolopyrimidine and tert-butylphenyl moieties. The modifications to compound 2 are mainly discussed with respect to the SAR, and it was expected to obtain a compound with excellent biological activity and PK properties.

2.3.2. Structural optimization of Compound 2

Based on compound 2, the linker between the pyrrolopyrimidine hinge binder and the warhead and the warhead itself were investigated (Table 6). Substitutions on the central phenyl ring were also investigated. Groups of compounds showed that both the 4-piperidine and the 4-tetrahydropyridine linker exhibited similar potency against BTK.

(34–39 vs. 2, 29–33), and the replacement of the acrylamido moiety with a but-2-ynamido moiety did not affect BTK potency. In addition, a smaller substituent (-F) was introduced to the R₄ site, and the high potency was retained. However, deleting the substituents on the phenyl ring caused an approximately 2-fold decrease in potency. Overall, all of

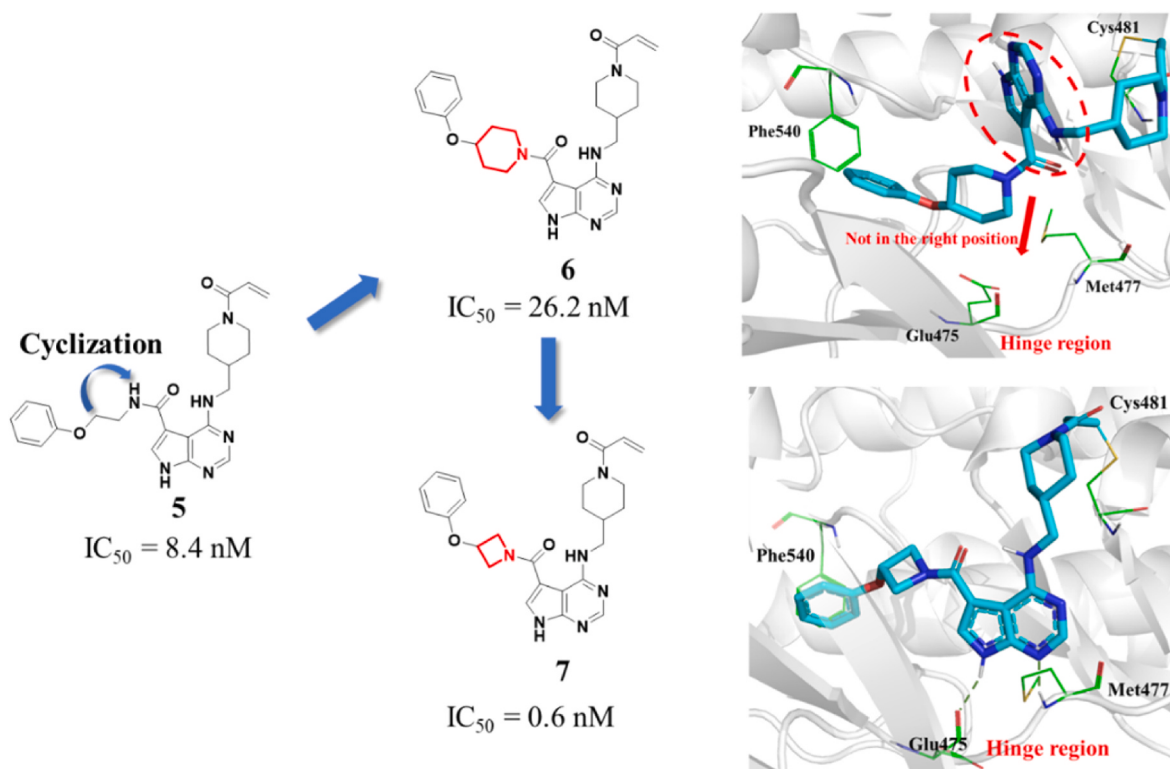


Fig. 3. Predicted binding mode of compounds **6** and **7** with BTK (PDB id: 5P9J). Compounds **6** and **7** are shown in cyan. Hydrogen bonds are displayed, and the amino acid residues are shown in green. The figures were generated using PyMOL (<http://www.pymol.org/>).

these compounds, with the exception of compound **33**, showed high potency with IC_{50} values below 10 nM. Compounds **2**, **29**, **30**, **31**, **34** and **37** were selected for activity testing in TMD8 cells, and the results showed that all of the tested compounds exhibited high potency that was comparable to ibrutinib and higher than that of evobrutinib (Table 4).

Further modifications were mainly focused on the R₆ site with the aim of reducing the size of the compounds (Table 7). First, compared with compound **2**, we kept the 4-piperidine linker unchanged but replaced the methyl substituent on the central phenyl ring with a fluoro group, considering that the fluoro might improve metabolic stability. For the R₆ site, the *tert*-butyl group was replaced with a cyclopropyl, yielding compounds **40** and **41** with retained high potency against BTK and in TMD8 cells. Furthermore, compound **42**, lacking the terminal phenyl substitution, even showed higher potency against BTK with an IC_{50} of 0.6 nM and comparable cellular potency. An aniline group was also introduced to the R₆ site, which caused a slight drop in potency in TMD8 cells (Table 4).

Due to the high cellular activity of this series of compounds, we first selected compound **42**, which had the smallest molecular weight, for PK study. In addition, compound **37** was selected, which was totally structurally different from **42**. The warhead of compound **37** bearing a *tert*-butyl moiety was a but-2-ynamido moiety, and the linker ring of the warhead was piperidine. Both **37** and **42** were selected for PK studies in mice following intravenous (2 mg/kg) and oral (10 mg/kg) administration. The study of **37** showed a low oral bioavailability of 0.78%. The low bioavailability of compound **37** may be because the *tert*-butyl group is easily oxidized in the liver [23]. To our delight, compound **42** showed a high oral bioavailability of 40.98%, which was higher than the oral bioavailability of other reported covalent inhibitors [11,24] (Table 5). In addition, after intravenous dosing at 2 mg/kg, the half-life ($t_{1/2}$) of **42** was 0.59 h, which was comparable to the reported half-life ($t_{1/2}$) of the covalent compounds. Taken together, these results show that modifying compound **2** successfully led to the generation of compound **42** with drug candidacy, which was selected for further profiling.

2.4. Kinase selectivity of compound **42**

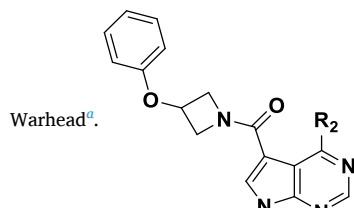
Compound **42** was screened at a 1 μM concentration to assess its kinase selectivity using DiscoverX's kinase scan technology (Fig. 4). Compound **42** possessed a high selectivity, as indicated by the selectivity S score (1) of 0.022 against 97 kinases and mutants tested at 1 μM . Only ERBB4 was inhibited at less than 1% of the control apart from BTK (Table S1). Compared with BTK, **42** showed weaker binding with JAK3 and EGFR, which contain cysteine residues in the same region of the receptor. Targeting wild-type (wt) EGFR is known to induce dramatic cutaneous toxicity and gastrointestinal adverse effects because the EGFR signaling cascade is involved in the biology of the skin and gastrointestinal system [25,26]. Ibrutinib has been reported to have 4.2-fold selectivity against EGFR, and zanubrutinib showed the slightly improved selectivity of 8.7-fold against EGFR, while compound **42** showed high selectivity for EGFR. Overall, **42** demonstrated an excellent selectivity profile against kinases.

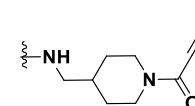
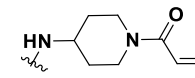
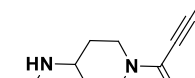
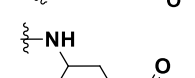
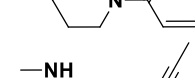
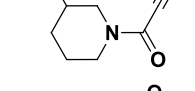
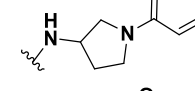
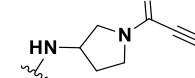
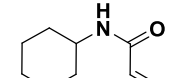
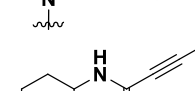
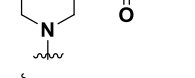
2.5. Antiproliferative activities of **42** against other B-cell lymphomas

We next evaluated the antiproliferative effects of compound **42** against a panel of B-cell lymphoma cell lines. As shown in Table 8, **42** exhibited potent antiproliferative activity against a human mantle cell lymphoma cell line (REC-1) with an IC_{50} value of 1.7 nM, suppressed the proliferation of DOHH2 cells in the micromolar range, while it was not potent against the other cell lines tested ($IC_{50} > 10 \mu\text{M}$). Ibrutinib suppressed the proliferation of SU-DHL-4 and DOHH2 cells with IC_{50} values of 0.804 μM and 0.5062 μM and suppressed the proliferation of Pfeiffer and Ramos cells in the micromolar range. It has been suggested that the survival of the TMD8 and REC-1 cell lines mainly relies on the BCR pathway, while other cells do not solely rely on this pathway for survival. This result confirmed that ibrutinib was a nonselective BTK inhibitor and that its antitumor activity was a consequence of multiple kinase inhibition, and illustrated the specificity of compound **42** for the

Table 2

Table 2
SAR for the warhead and linkers between the pyrrolopyrimidine core and



Compd.	R ₂	BTK IC ₅₀ (nM)
8		16.4
9		593.1
10		973.8
11		1.9
12		153.3
13		4.5
14		68.5
15		5410.2
16		>10000
17		2.2
18		92.9

^a Number of determinations = 1.

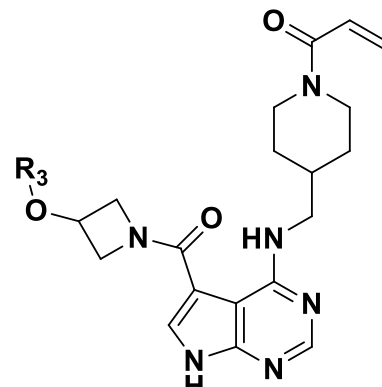
BCR pathway and its high kinase selectivity.

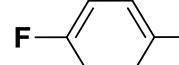
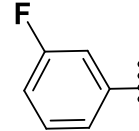
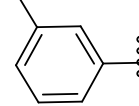
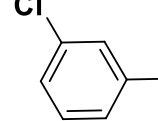
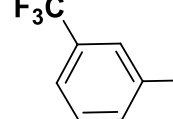
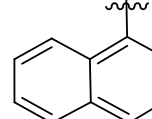
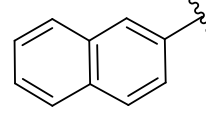
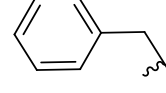
2.6. Effects of compound 42 on the signaling pathway

BTK plays an imperative role in the BCR signaling pathway, and the activation of BTK is marked by autophosphorylation of Tyr223, which is

Table 3

Table 3
SAR for terminal phenyl Optimization^a.



Compd.	R ₃	BTK IC ₅₀ (nM)
19		0.7
20		0.4
21		0.5
22		0.5
23		1.6
24		0.8
25		1.4
26		0.8
27		2.0
28		23.2

^a Number of determinations = 1.

Table 4Antiproliferative effects of selected compounds^a.

Compd.	TMD8 IC ₅₀ (nM)	Compd.	TMD8 IC ₅₀ (nM)	Compd.	TMD8 IC ₅₀ (nM)
2	1.5	23	22.4	37	1.8
7	24.4	24	22.6	40	0.8
11	454.5	25	28.0	41	1.2
13	2526	26	38.1	42	2.6 ^b
17	319.8	27	30.7	43	5.4
19	84.1	29	1.7	44	12.1
20	9.2	30	3.4	45	7.2
21	15.6	31	1.7	Ibrutinib	2.7
22	12.9	34	1.5	Evobrutinib	56.2

^a Number of determinations = 1.^b number of determinations = 2.

necessary for full activation of BTK. In BTK-dependent diffuse large B-cell lymphoma (DLBCL) TMD8 cancer cells, compound **42** was found to dose-dependently inhibit BTK autophosphorylation at the Tyr223 site with an IC₅₀ of 1.49 nM (Fig. 5).

2.7. Cell cycle arrest and induction of apoptosis by **42**

The effects of **42** on cell cycle progression in TMD8 cells were also investigated. After 48 h of treatment with TMD8 cells, **42** was found to significantly arrest cell cycle progression at G1 phase in a dose-dependent manner (Fig. 6A). Compared with 32.9% of the cells in G0/G1 phase in the control group, the percentage of cells in the G0/G1 phase increased from 33.0 to 63.0% when the concentration of compound **42** increased from 1 to 100 nM. The effects of **42** on apoptosis in TMD8 cells were also examined. As shown in Figs. 6B, **42** weakly triggered concentration-dependent apoptosis of the cells with values of 19%, 25.2%, and 31.4% at concentrations of 10 nM, 100 nM, and 1000 nM, respectively, compared with 18.2% in the untreated control cells. Together, these results demonstrated that **42**, as a new inhibitor of BTK, suppresses the growth of cancer cells mainly by G1 phase cell cycle arrest.

2.8. Safety profile of compound **42**

The safety profile of compound **42** was further evaluated. In the hERG inhibition assay, compound **42** showed low hERG channel activity with an IC₅₀ value of 4.38 μM, indicating that it had low potential for cardiotoxicity. We also studied the mutagenicity of **42** with a mini bacterial reverse mutation (AMES) test. Compound **42** was non-mutagenic at the tested concentrations (1.5–1000 μg/plate) with or without metabolic activation (using the five tester strains TA98, TA100, TA1535, TA1537 and WP2 uvrA (PKM101)). Single-dose toxicity studies were also performed with compound **42**, and the maximum tolerated doses (MTDs) were determined to be > 500 mg/kg. Overall, the preliminary toxicological results showed that compound **42** was a safe BTK inhibitor and, thus, could be a potential antitumor agent. (Details are displayed in Supporting Information).

Table 5Murine pharmacokinetic profiles of compounds **20**, **22**, **37** and **42**^a.

compd	route	dose, mg/kg	T _{max} , h	C _{max} , ng/ml	AUC _(0-t) , h·ng/ml	AUC _(0-∞) , h·ng/mL	T _{1/2} , h	Vz, l/kg	CL, l/h/kg	F, %
20	iv	2	0.03	2231.10	538.88	540.52	0.26	1.37	3.71	2.58
	po	10	0.25	148.04	69.48	75.31	0.95			
22	iv	2	0.05	1252.98	359.00	540.52	0.19	1.52	5.57	1.82
	po	10	0.11	48.61	32.75	32.94	0.39			
37	iv	2	0.03	2160.14	229.14	231.08	2.79	34.82	8.67	0.78
	po	10	0.08	49.93	8.94	9.57	1.39			
42	iv	2	0.03	2245.39	1471.35	718.33	0.67	2.79	2.87	40.98
	po	10	0.39	1441.59	718.33	1472.06	0.59			

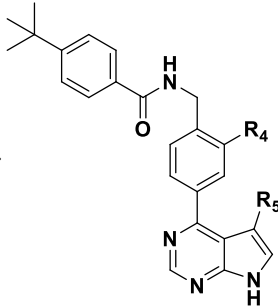
^a Three mice per study for iv and po administration. iv formulation: 2.5% DMSO/20% hydroxypropyl-β-cyclodextrin. po formulation: 0.5% CMC/water.

2.9. Tumor growth inhibition of **42** in the TMD8 xenograft model

To test the in vivo tumor growth inhibition of **42**, we evaluated its antitumor activity in female CB-17 SCID nude mice bearing human TMD8 tumor cells. Compound **42** was administered orally (po) at dosages of 12.5, 25, and 50 mg/kg twice daily (BID) for 21 consecutive days, while the control group was treated with ibrutinib at 25 mg/kg BID. As shown in Fig. 7A and Fig. 7B, oral administration of **42** at 12.5 mg/kg and 25 mg/kg showed significant antitumor efficacy that was comparable to ibrutinib, although the strong suppression was maintained for only 10 days. Administration of **42** at 50 mg/kg showed higher antitumor efficacy and not only completely inhibited tumor growth but also remarkably reduced tumor volume after 21 days with a TGI of 104%, which was slightly stronger than that of ibrutinib (103%). None of the animals in any of the treatment groups displayed significant weight fluctuations during the treatment course (Fig. 7C). The effects of **42** on target inhibition in tumors were also elucidated by using Western blot analysis. As illustrated in Figs. 7D, **42** showed a significant reduction in p-BTK (Tyr223) expression. These results clearly demonstrated that **42** efficiently inhibited the activation of BTK and thus suppressed tumor growth. The blood routine test of mice showed that administration of **42** at 50 mg/kg can reduce the content of white blood cells, lymphocytes and monocytes, while showed no effect on red blood cell and platelets, the same trend as Ibrutinib.

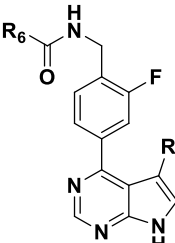
3. Conclusion

In summary, the binding mode of BTK inhibitors to BTK was first analyzed, and four key regions for binding were identified. Through an integrated drug design workflow that includes fragment-based methods for molecular generation and deep learning framework XgraphBoost for recognition and docking-based methods for visualization, we found four compounds that showed potency against BTK. Among them, compounds **1** and **2** bearing the same pyrrolopyrimidine core showed different binding modes and higher potency than pyrotinib and futibatinib. Further optimizations were based on compounds **1** and **2**. The optimization of compound **1** led us to obtain a series of BTK inhibitors with high inhibitory activity against BTK that exhibit robust efficacy in suppressing the growth of TMD8 cells. However, compounds **20** and **22** showed low oral bioavailability, and the evaluation could not be continued. Modification of compound **2** led to the discovery of compound **42**, which has the potential to be a novel therapeutic option for B-cell lymphomas. Compound **42** demonstrated excellent kinase selectivity, especially over EGFR kinase, indicating that off-target adverse effects may be prevented. Furthermore, the high oral bioavailability suggests a low dose requirement in clinical applications. Notably, compound **42** showed favorable safety in vivo. In TMD8 cell-derived animal xenograft models, **42** significantly inhibited tumor growth (TGI = 104%) at a dosage of 50 mg/kg, indicating its potential as a novel therapeutic option for B-cell lymphomas.

Table 6SAR of derivatives with different substituents at the R₄ and R₅


^a Number of determinations = 1.

Compd.	R ₄	R ₅	BTK IC ₅₀ (nM)
2	CH ₃		1.3
29	CH ₃		1.1
30	F		1.3
31	F		0.8
32	H		2.5
33	H		11.1
34	CH ₃		0.8
35	CH ₃		1.4
36	F		1.9
37	F		1.2
38	H		2.1
39	H		2.2

Table 7SAR of derivatives with different substituents at the R₅ and R₆


^a Number of determinations = 1.

Compd.	R ₅	R ₆	BTK IC ₅₀ (nM)
40			1.2
41			1.9
42			0.7 ^b
43			1.0
44			0.8
45			1.4

^a Number of determinations = 1.^b Number of determinations = 2.

from commercial sources and used without further purification. All air-sensitive reactions were carried out under an atmosphere of argon with magnetic stirring. Melting points were determined on Yanaco MP-J3 microscope melting point apparatus. ¹H NMR and ¹³C NMR spectra were recorded on Mercury-400, Mercury- 500, and Mercury-700 spectrometers at room temperature. Chemical shifts are referenced to the residual solvent peak and reported in ppm (δ scale), and all coupling constant (J) values are given in Hz. ESI-HRMS (ESI): M/Z data were measured on Thermo Exactive Orbitrap plus spectrometer. Flash column chromatography was performed on Biotage Isolera one. Purity of all compounds tested in biological assays was determined to be >95% by HPLC analysis, including the two purchased compounds. The following analytical method was used to determine chemical purity of final compounds: HPLC, Agilent ZORBAX SB C18, 5 μ m, 4.6 mm \times 150 mm. The column temperature was maintained at 25 °C, and the UV wavelength for detection was 254 nm. Method: using methanol as mobile phase A and water with 0.1% formic acid as mobile phase B at a flow rate of 1 mL/min, and the gradient program was as follows: 30% mobile phase A and 70% mobile phase B. (0–15min)

All final compounds passed the PAINS filter using False Positive Remover [27].

4.2. Chemistry

4.2.1. General synthetic procedure for compounds 1,3–28

To a solution of compound 47a–49k, 51a–53 (1.0 eq) in CH₂Cl₂ (2 mL) was added trifluoroacetic acid (1.0 mL) dropwise. The mixture was stirred at room temperature for 3h and then concentrated in vacuo. The

^a Number of determinations = 1.

4. Experimental

4.1. General information

Unless otherwise specified, all reagents and solvents were purchased

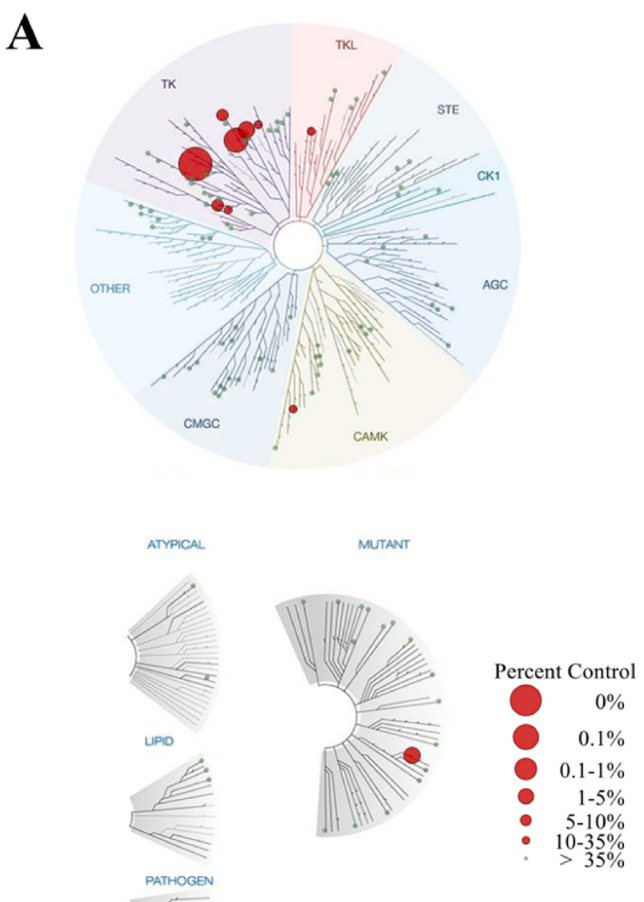


Fig. 4. Kinase selectivity profiling of **42** at 1 μ M (scanEDGE, DiscoverX). (A) TREESpot interaction maps for **42** against 97 kinases. (B) Results are reported as % of the control, where lower numbers indicate stronger hits in the matrix.

Table 8

Antiproliferative activities of **42** against other B-cell lymphomas.^a

Antiproliferative activity on B-cell lymphomas (IC_{50} , μ M)									
Compd	REC-1 ^b	Pfeiffer	OCI-LY3	SU-DHL-4	DOHH2 ^b	SU-DHL-6	Mino	Raji	Ramos ^b
42	0.0017	>10	>10	>10	5.263	>10	>10	>10	>10
Ibrutinib	0.0008	1.652	>10	0.804	0.5062	1.498	>10	>10	2.088

^a Number of determinations = 1.

^b number of determinations = 3.

crude product used in the next step without further purification. DIEA (3eq) was added to the solution of the crude product in dry DCM (2 mL) and stirred at -10°C for 5 min. Acryloyl chloride or 2-butynoyl chloride (1.2 eq) was added to the mixture. The mixture was stirred at rt for 3 h. After quenching with water and extracted with DCM (3 \times), the organic phase was separated and washed with brine, dried over Na_2SO_4 , filtered, and concentrated in vacuo. The residue was purified by silica column chromatography (DCM/MeOH) to afford the desired products **1–28**.

4-((1-acryloylpiperidin-4-yl)methyl)amino-N-phenethyl-7H-pyrrolo[2,3-d]pyridine-5-carboxamide (1). Compound **1** was prepared from compound **47a**. Yield: 49%. White solid. Mp: 189–191. ^1H NMR (400 MHz, DMSO-*d*₆) δ 12.01 (s, 1H), 9.67 (s, 1H), 8.47 (s, 1H), 8.11 (s, 1H), 7.87 (s, 1H), 7.41–7.10 (m, 5H), 6.79 (dd, *J* = 16.7, 10.3 Hz, 1H), 6.06 (d, *J* = 16.7 Hz, 1H), 5.62 (d, *J* = 10.5 Hz, 1H), 4.53–4.37 (m, 1H), 4.17–3.95 (m, 1H), 3.59–3.38 (m, 4H), 3.03 (t, *J* = 11.8 Hz, 1H), 2.90–2.84 (m, 2H), 2.69–2.55 (m, 1H), 1.95–1.83 (m, 1H), 1.82–1.67 (m, 2H), 1.30–1.02 (m, 2H). ^{13}C NMR (175 MHz, DMSO) δ 165.42, 164.64, 157.23, 153.25, 151.18, 139.98, 129.21, 129.13, 128.86, 127.38, 126.64, 124.47, 110.99, 101.43, 56.55, 45.54, 45.47,

41.92, 41.09, 36.46, 35.70, 31.02, 29.94, 19.08. HRMS (ESI): *m/z* calcd for $\text{C}_{24}\text{H}_{29}\text{N}_6\text{O}_2$ ($\text{M} + \text{H}$)⁺ 433.2351, found 433.2327. Purity: 100%.

4-((1-acryloylpiperidin-4-yl)methyl)amino-N-benzyl-7H-pyrrolo[2,3-d]pyrimidine-5-carboxamide (3). Compound **3** was prepared from compound **47b**. Yield: 52%. White solid. Mp: 160–163 °C.

^1H NMR (400 MHz, DMSO-*d*₆) δ 12.12 (s, 1H), 9.74 (s, 1H), 8.96 (s, 1H), 8.16 (s, 1H), 8.03 (s, 1H), 7.44–7.10 (m, 5H), 6.88–6.50 (m, 1H), 6.00 (t, *J* = 16.9 Hz, 1H), 5.66–5.44 (m, 1H), 4.48 (s, 2H), 4.25–3.79 (m, 2H), 3.80–3.57 (m, 1H), 3.52–3.35 (m, 2H), 2.00 (s, 1H), 1.89–1.44 (m, 3H).

^{13}C NMR (100 MHz, DMSO) δ 165.46, 164.61, 157.11, 153.12, 151.14, 139.99, 129.07, 128.80, 127.65, 127.34, 127.28, 124.82, 110.74, 101.41, 45.44, 42.72, 41.86, 36.39, 30.95, 29.88, 29.48. HRMS (ESI): *m/z* calcd for $\text{C}_{23}\text{H}_{27}\text{N}_6\text{O}_2$ ($\text{M} + \text{H}$)⁺ 419.2186, found 419.2187. Purity: 99.8%.

4-((1-acryloylpiperidin-4-yl)methyl)amino-N-benzyl-7H-pyrrolo[2,3-d]pyrimidine-5-carboxamide (4). Compound **4** was prepared from compound **47c**. Yield: 48%. White solid. Mp: 138–140 °C. ^1H NMR (400 MHz, DMSO-*d*₆) δ 12.19 (s, 1H), 9.97 (s, 1H), 9.29 (t, *J* = 5.9

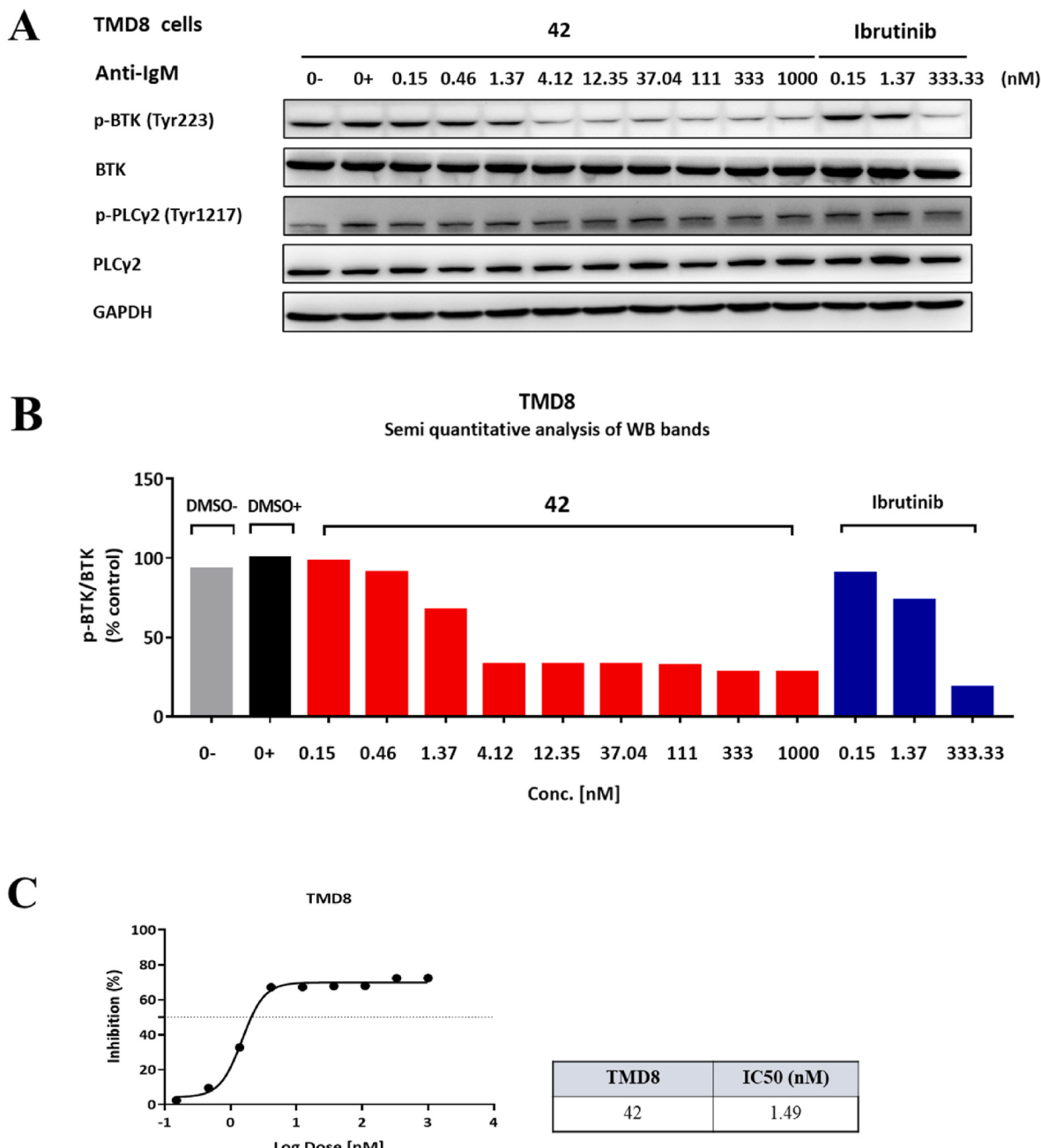


Fig. 5. Compound 42 blocked autophosphorylation of BTK (Tyr223) in TMD8 cells. (A) Western blot analysis of the inhibition of BTK (Tyr223) by compound 42 in TMD8 cells. (B) Semiquantitative analysis of BTK (Tyr223) autophosphorylation inhibition by compound 42 in TMD8 cells. (C) Dose-dependence curve and IC₅₀ of 42 in BTK-autophosphorylated TMD8 cells.

Hz, 1H), 8.19–8.12 (m, 1H), 8.10 (s, 1H), 7.68–7.54 (m, 2H), 7.31 (t, J = 7.9 Hz, 2H), 7.06 (t, J = 7.4 Hz, 1H), 6.74 (dd, J = 16.7, 10.4 Hz, 1H), 6.01 (dd, J = 16.7, 2.5 Hz, 1H), 5.58 (dd, J = 10.4, 2.5 Hz, 1H), 4.38 (d, J = 13.0 Hz, 1H), 4.07–3.92 (m, 1H), 3.40 (q, J = 6.7 Hz, 2H), 2.97 (t, J = 13.5 Hz, 1H), 2.57 (t, J = 12.6 Hz, 1H), 1.91–1.79 (m, 1H), 1.73 (t, J = 10.2 Hz, 2H), 1.15–0.94 (m, 2H). ¹³C NMR (175 MHz, DMSO) δ 163.77, 163.58, 156.39, 152.62, 150.69, 138.37, 128.33, 128.27, 126.52, 125.34, 123.37, 120.52, 110.08, 44.66, 41.05, 35.57, 30.14, 29.05. HRMS (ESI): m/z calcd for C₂₂H₂₅N₆O₂ (M + H)⁺ 405.2035, found 405.2018. Purity: 100%.

4-((1-acryloylpiperidin-4-yl)methyl)amino)-N-(2-phenoxyethyl)-7*H*-pyrrolo [2,3-d] pyrimidine-5-carboxamide (**5**). Compound **5** was prepared from compound **47d**. Yield: 50%. White solid. Mp: 219–220 °C. ¹H NMR (400 MHz, DMSO-*d*₆) δ 12.07 (s, 1H), 9.68 (t,

J = 5.9 Hz, 1H), 8.65 (t, J = 5.6 Hz, 1H), 8.11 (s, 1H), 7.97 (s, 1H), 7.39–7.23 (m, 2H), 7.01–6.88 (m, 3H), 6.79 (dd, J = 16.7, 10.5 Hz, 1H), 6.06 (dd, J = 16.7, 2.5 Hz, 1H), 5.63 (dd, J = 10.5, 2.5 Hz, 1H), 4.43 (d, J = 13.0 Hz, 1H), 4.15–3.92 (m, 3H), 3.64 (q, J = 5.7 Hz, 2H), 3.42 (q, J = 6.4 Hz, 2H), 3.02 (t, J = 12.9 Hz, 1H), 2.62 (t, J = 12.5 Hz, 1H), 1.93–1.86 (m, 1H), 1.78 (t, J = 9.6 Hz, 2H), 1.22–1.00 (m, 2H). ¹³C NMR (100 MHz, DMSO) δ 165.78, 164.60, 158.87, 157.08, 153.11, 151.13, 130.00, 129.09, 127.31, 124.88, 121.15, 114.94, 110.70, 101.37, 66.49, 53.93, 45.47, 41.86, 39.18, 36.39, 30.96, 29.88, 18.50, 17.19, 12.84. HRMS (ESI): m/z calcd for C₂₄H₂₉N₆O₃ (M + H)⁺ 449.2283, found 449.2285. Purity: 100%.

1-(4-(((5-(4-phenoxy)piperidine-1-carbonyl)-7*H*-pyrrolo [2,3-d] pyrimidin-4-yl)amino)methyl)piperidin-1-ylprop-2-en-1-one (**6**). Compound **6** was prepared from compound **48**. Yield: 45%. White solid.

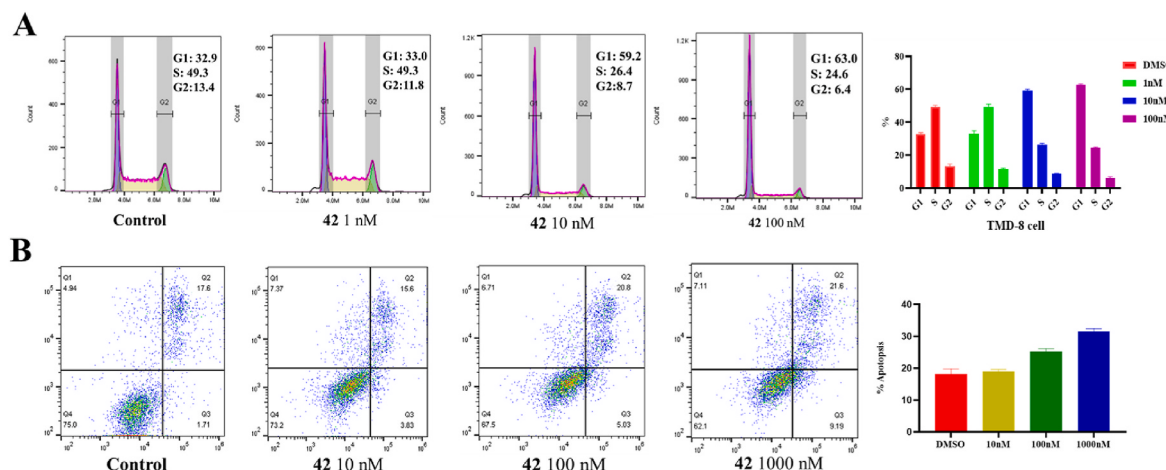


Fig. 6. (A) Effects of **42** on the cell cycle in TMD8 cells. Compound **42** induced apoptosis of TMD8 cells. TMD8 cells were treated with 1, 10, and 100 nm compound **42** for 48 h. (B) Compound **42** induced apoptosis of TMD8 cells. TMD8 cells were treated with 10, 100, and 1000 nm compound **42** for 72 h. Data are shown as the mean \pm SD. Each experiment was conducted independently twice.

Mp: 96–98 °C. ^1H NMR (400 MHz, DMSO-*d*₆) δ 12.14 (s, 1H), 8.23–8.09 (m, 2H), 7.58 (s, 1H), 7.29 (t, *J* = 7.7 Hz, 2H), 7.00 (d, *J* = 8.0 Hz, 2H), 6.93 (t, *J* = 7.3 Hz, 1H), 6.79 (dd, *J* = 16.7, 10.4 Hz, 1H), 6.07 (dd, *J* = 16.7, 2.5 Hz, 1H), 5.63 (dd, *J* = 10.4, 2.5 Hz, 1H), 4.69 (tt, *J* = 7.7, 3.6 Hz, 1H), 4.50–4.35 (m, 1H), 4.12–3.96 (m, 3H), 3.68–3.53 (m, 2H), 3.48–3.35 (m, 2H), 3.02 (t, *J* = 12.9 Hz, 1H), 2.61 (t, *J* = 12.4 Hz, 1H), 2.06–1.97 (m, 2H), 1.93–1.84 (m, 1H), 1.81–1.61 (m, 4H), 1.24–1.04 (m, 2H). ^{13}C NMR (100 MHz, DMSO) δ 166.48, 164.57, 157.35, 157.05, 153.07, 150.91, 130.07, 129.07, 127.33, 125.14, 121.23, 116.37, 108.24, 102.16, 71.98, 45.47, 41.86, 36.32, 31.16, 30.90, 29.82. HRMS (ESI): *m/z* calcd for C₂₇H₃₃N₆O₃ (M + H)⁺ 489.2630, found 489.2628. Purity: 100%.

1-(4-((5-(3-phenoxyazetidine-1-carbonyl)-7*H*-pyrrolo[2,3-d]pyrimidin-4-yl)amino)methyl)piperidin-1-yl)prop-2-en-1-one (7). Compound **7** was prepared from compound **49a**. Yield: 50%. White solid. Mp: 178–181 °C. ^1H NMR (500 MHz, DMSO-*d*₆) δ 12.24 (s, 1H), 9.53 (s, 1H), 8.13 (s, 1H), 7.66 (s, 1H), 7.33 (t, *J* = 7.7 Hz, 2H), 7.01 (t, *J* = 7.5 Hz, 1H), 6.88 (d, *J* = 8.0 Hz, 2H), 6.79 (dd, *J* = 16.7, 10.5 Hz, 1H), 6.06 (d, *J* = 15.9 Hz, 1H), 5.63 (d, *J* = 10.3 Hz, 1H), 5.12 (s, 1H), 4.92 (s, 1H), 4.55 (s, 2H), 4.43 (d, *J* = 13.1 Hz, 1H), 4.06 (d, *J* = 14.2 Hz, 2H), 3.57–3.35 (m, 2H), 3.03 (t, *J* = 13.2 Hz, 1H), 2.63 (t, *J* = 12.8 Hz, 1H), 1.92–1.84 (m, 1H), 1.78 (t, *J* = 13.3 Hz, 2H), 1.21–0.97 (m, 2H). ^{13}C NMR (100 MHz, DMSO) δ 166.40, 164.59, 157.20, 156.80, 153.47, 151.08, 130.28, 129.09, 127.34, 126.52, 121.87, 115.10, 108.38, 101.48, 66.52, 45.49, 41.85, 36.36, 31.43, 30.97, 29.89, 22.54, 19.03, 14.44. HRMS (ESI): *m/z* calcd for C₂₅H₂₉N₆O₃ (M + H)⁺ 461.2298, found 461.2298. Purity: 100%.

1-(4-((5-(3-phenoxyazetidine-1-carbonyl)-7*H*-pyrrolo[2,3-d]pyrimidin-4-yl)amino)methyl)piperidin-1-yl)but-2-yn-1-one (8). Compound **8** was prepared from compound **49a**. Yield: 46%. yellow solid. Mp: 230–232 °C. ^1H NMR (400 MHz, DMSO-*d*₆) δ 12.22 (s, 1H), 9.49 (t, *J* = 5.8 Hz, 1H), 8.09 (s, 1H), 7.62 (s, 1H), 7.29 (t, *J* = 7.8 Hz, 2H), 6.96 (t, *J* = 7.3 Hz, 1H), 6.84 (d, *J* = 8.1 Hz, 2H), 5.08 (tt, *J* = 6.3, 3.4 Hz, 1H), 4.87 (s, 1H), 4.51 (s, 2H), 4.37–4.14 (m, 2H), 3.98 (q, *J* = 7.1 Hz, 1H), 3.49–3.29 (m, 2H), 3.05 (t, *J* = 11.5 Hz, 1H), 2.60 (t, *J* = 11.3 Hz, 1H), 1.96 (s, 3H), 1.90–1.59 (m, 3H), 1.23–1.10 (m, 1H), 1.03–1.01 (m, 1H). ^{13}C NMR (100 MHz, DMSO) δ 166.39, 157.18, 156.80, 153.46, 152.25, 151.08, 130.28, 126.55, 121.88, 115.10, 108.38, 101.48, 89.48, 73.59, 66.51, 46.71, 45.36, 40.92, 36.29, 30.63, 29.63, 3.78. HRMS (ESI): *m/z* calcd. for C₂₆H₂₉N₆O₃ (M + H)⁺ 473.2308, found 473.2219. Purity: 95.9%.

1-(4-((5-(3-phenoxyazetidine-1-carbonyl)-7*H*-pyrrolo[2,3-d]pyrimidin-4-yl)amino)methyl)piperidin-1-yl)prop-2-en-1-one (9). Compound **9** was prepared from compound **51a**. Yield: 43%. White solid.

Mp: 148–150 °C. ^1H NMR (400 MHz, DMSO-*d*₆) δ 12.28 (s, 1H), 9.61 (d, *J* = 7.4 Hz, 1H), 8.16 (s, 1H), 7.68 (s, 1H), 7.39–7.27 (m, 2H), 7.05–6.95 (m, 1H), 6.92–6.86 (m, 2H), 6.86–6.79 (m, 1H), 6.10 (dd, *J* = 16.7, 2.4 Hz, 1H), 5.67 (dd, *J* = 10.5, 2.5 Hz, 1H), 5.17–5.03 (m, 1H), 4.99–4.83 (m, 1H), 4.67–4.45 (m, 2H), 4.38–4.21 (m, 1H), 4.18–3.83 (m, 3H), 3.38 (t, *J* = 12.0 Hz, 1H), 3.14 (t, *J* = 11.5 Hz, 1H), 2.12–1.95 (m, 2H), 1.57–1.31 (m, 2H). ^{13}C NMR (100 MHz, DMSO) δ 166.38, 164.81, 156.80, 156.22, 153.48, 151.17, 130.27, 129.01, 127.53, 126.68, 121.87, 115.09, 108.33, 101.57, 66.51, 46.43, 44.00, 32.78, 31.77. HRMS (ESI): *m/z* calcd for C₂₄H₂₇N₆O₃ (M + H)⁺ 447.2157, found 447.2158. Purity: 100%.

1-(4-((5-(3-phenoxyazetidine-1-carbonyl)-7*H*-pyrrolo[2,3-d]pyrimidin-4-yl)amino)methyl)piperidin-1-yl)but-2-yn-1-one (10). Compound **10** was prepared from compound **51a**. Yield: 44%. White solid. Mp: 243–245 °C. ^1H NMR (400 MHz, DMSO-*d*₆) δ 12.30 (s, 1H), 9.63 (s, 1H), 8.16 (s, 1H), 7.68 (s, 1H), 7.34–7.32 (m, 2H), 7.08–6.95 (m, 1H), 6.93–6.80 (m, 2H), 5.19–5.06 (m, 1H), 4.97–4.85 (m, 1H), 4.69–4.48 (m, 2H), 4.39–4.23 (m, 1H), 4.17–3.84 (m, 3H), 3.60–3.42 (m, 1H), 3.22–3.08 (m, 1H), 2.18–1.81 (m, 5H), 1.55–1.11 (m, 2H). ^{13}C NMR (100 MHz, DMSO) δ 166.38, 156.79, 156.20, 153.47, 152.38, 151.17, 130.27, 126.72, 121.87, 115.09, 108.32, 101.58, 89.71, 73.46, 66.51, 46.33, 45.18, 39.44, 32.42, 31.47, 3.83. HRMS (ESI): *m/z* calcd for C₂₅H₂₇N₆O₃ (M + H)⁺ 459.2155, found 459.2144. Purity: 100%.

1-(3-((5-(3-phenoxyazetidine-1-carbonyl)-7*H*-pyrrolo[2,3-d]pyrimidin-4-yl)amino)methyl)piperidin-1-yl)prop-2-en-1-one (11). Compound **11** was prepared from compound **51b**. Yield: 51%. White solid. Mp: 228–230 °C. ^1H NMR (500 MHz, DMSO-*d*₆) δ 12.27 (s, 1H), 9.57 (s, 1H), 8.18 (s, 1H), 7.67 (s, 1H), 7.32 (d, *J* = 7.9 Hz, 2H), 7.00 (t, *J* = 7.6 Hz, 1H), 6.88 (d, *J* = 8.0 Hz, 2H), 6.56 (s, 1H), 6.13–5.82 (m, 1H), 5.73–5.40 (m, 1H), 5.12 (s, 1H), 4.90 (s, 1H), 4.54 (s, 2H), 4.25–3.83 (m, 3H), 3.75–3.58 (m, 1H), 3.52–3.36 (m, 2H), 2.01 (s, 1H), 1.88–1.45 (m, 3H). ^{13}C NMR (100 MHz, DMSO) δ 166.32, 165.00, 156.79, 156.36, 153.45, 151.16, 130.28, 129.26, 128.73, 127.21, 126.68, 121.87, 115.10, 108.34, 101.60, 66.51, 49.79, 46.92, 46.53, 45.92, 42.36, 30.59, 30.11, 29.50, 24.11, 22.87. HRMS (ESI): *m/z* calcd for C₂₄H₂₇N₆O₃ (M + H)⁺ 447.2152, found 447.2152. Purity: 96.8%.

1-(3-((5-(3-phenoxyazetidine-1-carbonyl)-7*H*-pyrrolo[2,3-d]pyrimidin-4-yl)amino)methyl)piperidin-1-yl)but-2-yn-1-one (12). Compound **12** was prepared from compound **51b**. Yield: 46%. White solid. Mp: 153–155 °C. ^1H NMR (500 MHz, DMSO-*d*₆) δ 12.36 (s, 1H), 9.76 (s, 1H), 8.22 (s, 1H), 7.71 (s, 1H), 7.33 (t, *J* = 7.8 Hz, 2H), 7.01 (t, *J* = 7.5 Hz, 1H), 6.88 (d, *J* = 8.0 Hz, 2H), 5.13 (s, 1H), 4.92 (s, 1H), 4.56 (s, 2H), 4.12 (s, 1H), 4.07–3.75 (m, 3H), 3.70–3.47 (m, 1H), 3.46–3.15 (m, 1H), 2.01 (s, 3H), 1.89–1.70 (m, 1H), 1.68–1.61 (m, 2H), 1.58–1.47 (m, 1H).

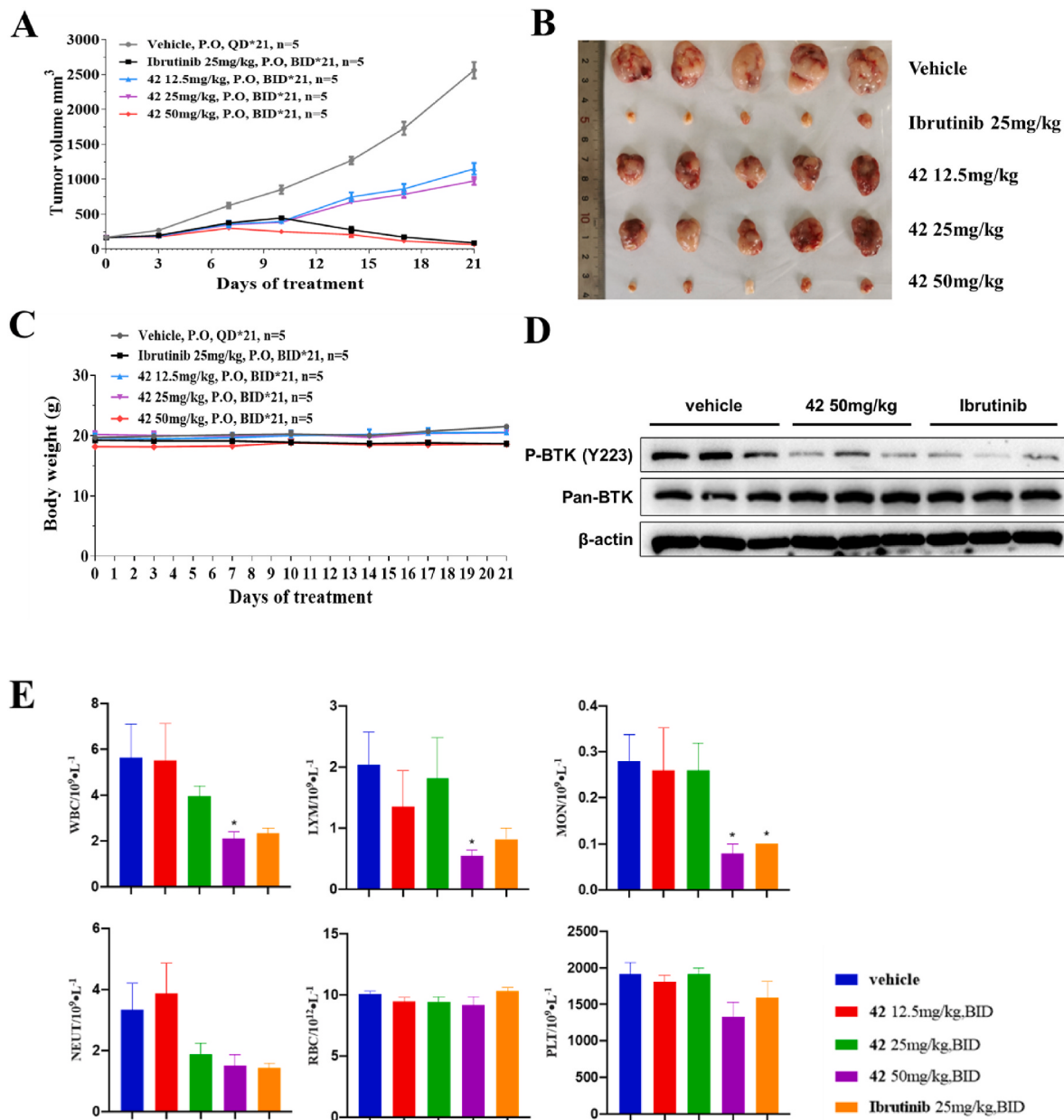


Fig. 7. In vivo TMD8 xenograft model study of compound 42. (A) The tumor volume curve of the five groups, including vehicle control, ibrutinib (25 mg/kg, BID), 42 (12.5 mg/kg, BID), 42 (25 mg/kg, BID), and 42 (50 mg/kg, BID). All animals were euthanized on day 22 of treatment. (B) Images of isolated subcutaneous xenograft tumors are shown on the day after the mice completed the treatment course with compound 42. (C) Body weight changes in the animals in the five groups over time. (D) Inhibition of BTK activation by 42 in tumors. (E) Summary of indicators from blood routine test for test compounds (Mean \pm SD, n = 5).

^{13}C NMR (100 MHz, DMSO) δ 166.19, 166.17, 156.79, 156.77, 152.73, 150.87, 150.72, 130.27, 127.00, 126.88, 121.87, 115.10, 108.65, 108.62, 101.78, 101.58, 89.65, 88.73, 73.57, 73.34, 66.51, 50.39, 46.89, 46.49, 45.95, 45.35, 41.48, 30.28, 29.60, 23.62, 22.13, 3.81, 3.21. HRMS (ESI): m/z calcd for $\text{C}_{25}\text{H}_{27}\text{N}_6\text{O}_3$ ($\text{M} + \text{H}$) $^+$ 459.2140, found 459.2152. Purity: 98.7%.

1-(3-((5-(3-phenoxyazetidine-1-carbonyl)-7*H*-pyrrolo[2,3-*d*]pyrimidin-4-yl)amino)pyrrolidin-1-yl)prop-2-en-1-one (13). Compound 13 was prepared from compound 51c. Yield: 45%. White solid. Mp: 138–140 °C.

^1H NMR (400 MHz, DMSO- d_6) δ 12.36 (s, 1H), 9.78 (s, 1H), 8.20 (s, 1H), 7.70 (s, 1H), 7.42–7.25 (m, 2H), 7.00 (t, J = 7.3 Hz, 1H), 6.87 (d, J = 8.1 Hz, 2H), 6.70–6.46 (m, 1H), 6.21–6.06 (m, 1H), 5.75–5.57 (m, 1H), 5.11 (tt, J = 6.2, 3.4 Hz, 1H), 4.98–4.84 (m, 1H), 4.76–4.62 (m, 1H), 4.65–4.43 (m, 2H), 4.09–3.87 (m, 1H), 3.79–3.68 (m, 1H), 3.56 (t,

J = 7.1 Hz, 1H), 3.51–3.36 (m, 2H), 2.37–2.11 (m, 1H), 2.05–1.80 (m, 1H).

^{13}C NMR (100 MHz, DMSO) δ 166.35, 166.30, 163.98, 156.79, 130.28, 130.09, 129.76, 127.38, 127.29, 126.94, 121.87, 115.10, 108.34, 101.70, 101.67, 66.51, 53.99, 52.47, 51.95, 50.60, 49.02, 44.90, 44.37, 31.98, 30.25, 18.53, 17.20. HRMS (ESI): m/z calcd for $\text{C}_{23}\text{H}_{25}\text{N}_6\text{O}_3$ ($\text{M} + \text{H}$) $^+$ 433.2018, found 433.2020. Purity: 100%.

1-(3-((5-(3-phenoxyazetidine-1-carbonyl)-7*H*-pyrrolo[2,3-*d*]pyrimidin-4-yl)amino)pyrrolidin-1-yl)but-2-yn-1-one (14). Compound 14 was prepared from compound 51c. Yield: 42%. White solid. Mp: 155–157 °C. ^1H NMR (400 MHz, DMSO- d_6) δ 12.29 (s, 1H), 9.69 (t, J = 7.1 Hz, 1H), 8.16 (s, 1H), 7.65 (t, J = 2.4 Hz, 1H), 7.33–7.18 (m, 2H), 6.95 (t, J = 7.4 Hz, 1H), 6.83 (d, J = 8.1 Hz, 2H), 5.07 (tt, J = 6.6, 3.6 Hz, 1H), 4.95–4.76 (m, 1H), 4.66–4.41 (m, 3H), 4.04–3.86 (m, 1H), 3.76–3.56 (m, 1H), 3.44 (t, J = 7.2 Hz, 2H), 2.34–2.17 (m, 1H), 1.95 (d,

$J = 17.1$ Hz, 4H). ^{13}C NMR (100 MHz, DMSO) δ 166.36, 166.32, 156.80, 156.44, 153.41, 152.36, 152.24, 151.14, 130.28, 130.25, 126.93, 121.87, 115.10, 108.28, 101.70, 88.30, 88.07, 74.84, 74.74, 66.52, 53.86, 51.34, 49.83, 49.42, 46.33, 43.78, 31.43, 31.33, 30.56, 22.54, 14.44, 3.71, 3.67. HRMS (ESI): m/z calcd for $\text{C}_{24}\text{H}_{25}\text{N}_6\text{O}_3$ ($\text{M} + \text{H}$) $^+$ 445.2026, found 445.2026. Purity: 96.8%.

N-(1-(5-(3-phenoxyazetidine-1-carbonyl)-7H-pyrrolo[2,3-d]pyrimidin-4-yl)pip eridin-3-yl)acrylamide (15).

Compound 15 was prepared from compound 52. Yield: 45%. White solid. Mp: 142–143 °C. ^1H NMR (500 MHz, DMSO- d_6) δ 12.16 (s, 1H), 8.24 (s, 1H), 8.16–7.90 (m, 1H), 7.61 (s, 1H), 7.30 (t, $J = 7.9$ Hz, 2H), 6.98 (t, $J = 7.5$ Hz, 1H), 6.82 (d, $J = 8.0$ Hz, 2H), 6.29–6.16 (m, 1H), 6.14–6.01 (m, 1H), 5.55 (d, $J = 10.1$ Hz, 1H), 5.08–4.87 (m, 1H), 4.60–4.38 (m, 2H), 4.26–4.07 (m, 2H), 4.06–3.88 (m, 2H), 3.89–3.62 (m, 1H), 3.05–2.76 (m, 2H), 2.06–1.90 (m, 1H), 1.82–1.72 (m, 1H), 1.71–1.55 (m, 1H), 1.52–1.40 (m, 1H). ^{13}C NMR (100 MHz, DMSO) δ 164.53, 156.78, 153.36, 151.48, 132.12, 130.25, 125.74, 125.30, 125.07, 121.82, 115.01, 109.28, 66.08, 58.98, 52.82, 48.18, 46.43, 30.62, 23.62. HRMS (ESI): m/z calcd for $\text{C}_{24}\text{H}_{27}\text{N}_6\text{O}_3$ ($\text{M} + \text{H}$) $^+$ 447.2168, found 447.2168. Purity: 100%.

N-(1-(5-(3-phenoxyazetidine-1-carbonyl)-7H-pyrrolo[2,3-d]pyrimidin-4-yl)pip eridin-3-yl)but-2-ynamide (16).

Compound 16 was prepared from compound 52. Yield: 42%. White solid. Mp: 140–142 °C. ^1H NMR (500 MHz, DMSO- d_6) δ 12.18 (s, 1H), 8.63–8.37 (m, 1H), 8.24 (s, 1H), 7.61 (s, 1H), 7.31 (t, $J = 7.7$ Hz, 2H), 6.98 (t, $J = 7.4$ Hz, 1H), 6.85 (d, $J = 7.9$ Hz, 2H), 5.10–4.99 (m, 1H), 4.58–4.34 (m, 2H), 4.22–3.85 (m, 4H), 3.84–3.59 (m, 1H), 2.99–2.72 (m, 2H), 2.04–1.81 (m, 4H), 1.77–1.37 (m, 3H). ^{13}C NMR (100 MHz, DMSO) δ 166.56, 158.67, 156.81, 153.33, 152.34, 151.48, 130.26, 125.38, 125.07, 121.83, 114.99, 109.27, 101.49, 83.05, 76.10, 66.13, 58.94, 55.35, 52.35, 48.09, 46.71, 46.30, 30.12, 29.49, 27.03, 25.58, 23.57, 22.57, 14.43, 3.44. HRMS (ESI): m/z calcd for $\text{C}_{25}\text{H}_{27}\text{N}_6\text{O}_3$ ($\text{M} + \text{H}$) $^+$ 459.2169, found 459.2169. Purity: 95.6%.

1-(4-hydroxy-4-((5-(3-phenoxyazetidine-1-carbonyl)-7H-pyrrolo[2,3-d]pyrimidin-4-yl)amino)methyl)piperidin-1-yl)prop-2-en-1-one (17). Compound 17 was prepared from compound 53. Yield: 36%. White solid. Mp: 140–141 °C. ^1H NMR (400 MHz, DMSO- d_6) δ 12.26 (s, 1H), 9.58 (t, $J = 5.8$ Hz, 1H), 8.11 (s, 1H), 7.67 (s, 1H), 7.33 (dd, $J = 8.6$, 7.3 Hz, 2H), 7.01 (dd, $J = 7.9$, 6.8 Hz, 1H), 6.91–6.86 (m, 2H), 6.79 (dd, $J = 16.7$, 10.5 Hz, 1H), 6.06 (dd, $J = 16.7$, 2.5 Hz, 1H), 5.62 (dd, $J = 10.4$, 2.5 Hz, 1H), 5.20–5.09 (m, 1H), 4.98–4.86 (m, 2H), 4.70–4.39 (m, 2H), 4.17–4.06 (m, 1H), 4.07–3.89 (m, 1H), 3.86–3.71 (m, 1H), 3.58–3.50 (m, 2H), 3.42–3.33 (m, 1H), 3.11–2.90 (m, 1H), 1.66–1.34 (m, 4H). ^{13}C NMR (100 MHz, DMSO) δ 166.29, 164.50, 157.53, 156.80, 153.25, 151.12, 130.27, 129.01, 127.33, 126.50, 121.87, 115.10, 108.54, 101.44, 69.49, 66.52, 50.46, 41.74, 38.13, 35.80, 34.78. HRMS (ESI): m/z calcd for $\text{C}_{25}\text{H}_{29}\text{N}_6\text{O}_4$ ($\text{M} + \text{H}$) $^+$ 477.2254, found 477.2256. Purity: 98.0%.

N-(2-((5-(3-phenoxyazetidine-1-carbonyl)-7H-pyrrolo[2,3-d]pyrimidin-4-yl)amino)ethyl)acrylamide (18). Compound 18 was prepared from compound 51d. Yield: 42%. White solid. Mp: 139–140 °C. ^1H NMR (400 MHz, DMSO- d_6) δ 12.28 (s, 1H), 9.48 (t, $J = 5.5$ Hz, 1H), 8.28 (t, $J = 5.5$ Hz, 1H), 8.16 (s, 1H), 7.68 (s, 1H), 7.33 (t, $J = 7.8$ Hz, 2H), 7.01 (t, $J = 7.3$ Hz, 1H), 6.88 (d, $J = 8.0$ Hz, 2H), 6.21 (dd, $J = 17.0$, 10.1 Hz, 1H), 6.07 (dd, $J = 17.2$, 2.3 Hz, 1H), 5.57 (dd, $J = 10.1$, 2.3 Hz, 1H), 5.20–5.07 (m, 1H), 5.00–4.81 (m, 1H), 4.68–4.38 (m, 2H), 4.13–3.90 (m, 1H), 3.66–3.52 (m, 2H), 3.42–3.32 (m, 2H). ^{13}C NMR (100 MHz, DMSO) δ 166.36, 165.32, 157.15, 156.79, 153.39, 151.13, 132.30, 130.29, 126.56, 125.46, 121.88, 115.11, 108.39, 101.64, 66.51, 39.02. HRMS (ESI): m/z calcd for $\text{C}_{21}\text{H}_{23}\text{N}_6\text{O}_3$ ($\text{M} + \text{H}$) $^+$ 407.1820, found 407.1822. Purity: 100%.

1-(4-((5-(3-(4-fluorophenoxy)azetidine-1-carbonyl)-7H-pyrrolo[2,3-d]pyrimidin-4-yl)amino)methyl)piperidin-1-yl)prop-2-en-1-one (19). Compound 19 was prepared from compound 49b. Yield: 40%. White solid. Mp: 184–186 °C. ^1H NMR (400 MHz, DMSO- d_6) δ 12.26 (s, 1H), 9.52 (t, $J = 5.7$ Hz, 1H), 8.14 (s, 1H), 7.66 (s, 1H), 7.16 (t, $J = 8.8$ Hz, 2H), 6.97–6.86 (m, 2H), 6.79 (dd, $J = 16.7$, 10.5 Hz, 1H),

6.07 (dd, $J = 16.7$, 2.5 Hz, 1H), 5.63 (dd, $J = 10.4$, 2.5 Hz, 1H), 5.09 (tt, $J = 6.7$, 3.8 Hz, 1H), 4.97–4.81 (m, 1H), 4.67–4.48 (m, 2H), 4.48–4.31 (m, 1H), 4.12–3.95 (m, 2H), 3.50–3.35 (m, 2H), 3.02 (t, $J = 12.8$ Hz, 1H), 2.62 (t, $J = 12.6$ Hz, 1H), 1.91–1.84 (m, 1H), 1.83–1.71 (m, 2H), 1.20–1.03 (m, 2H). ^{13}C NMR (100 MHz, DMSO) δ 166.36, 165.31, 157.15, 156.79, 153.39, 151.13, 132.30, 130.29, 126.56, 125.46, 121.88, 115.11, 108.39, 101.64, 66.51, 39.02. HRMS (ESI): m/z calcd for $\text{C}_{25}\text{H}_{28}\text{FN}_6\text{O}_3$ ($\text{M} + \text{H}$) $^+$ 479.2208, found 479.2209. Purity: 100%.

1-(4-((5-(3-(3-fluorophenoxy)azetidine-1-carbonyl)-7H-pyrrolo[2,3-d]pyramid in-4-yl)amino)methyl)piperidin-1-yl)prop-2-en-1-one (20). Compound 20 was prepared from compound 49c. Yield: 45%. White solid. Mp: 170–171 °C. ^1H NMR (400 MHz, DMSO- d_6) δ 12.26 (s, 1H), 9.51 (t, $J = 5.7$ Hz, 1H), 8.13 (s, 1H), 7.66 (s, 1H), 7.42–7.27 (m, 1H), 6.91–6.61 (m, 4H), 6.06 (dd, $J = 16.7$, 2.5 Hz, 1H), 5.63 (dd, $J = 10.4$, 2.5 Hz, 1H), 5.14 (tt, $J = 6.6$, 3.7 Hz, 1H), 4.99–4.85 (m, 1H), 4.66–4.50 (m, 2H), 4.48–4.31 (m, 1H), 4.14–3.96 (m, 2H), 3.54–3.37 (m, 2H), 3.02 (t, $J = 12.9$ Hz, 1H), 2.62 (t, $J = 12.6$ Hz, 1H), 1.92–1.82 (m, 1H), 1.83–1.70 (m, 2H), 1.20–1.01 (m, 2H). ^{13}C NMR (100 MHz, DMSO) δ 166.41, 164.73, 164.59, 162.31, 158.29, 158.18, 157.19, 153.48, 151.09, 131.61, 131.51, 129.09, 127.34, 126.56, 111.52, 111.50, 108.70, 108.49, 108.33, 102.95, 102.70, 101.46, 67.02, 45.49, 41.85, 36.36, 30.97, 29.89. HRMS (ESI): m/z calcd for $\text{C}_{25}\text{H}_{28}\text{FN}_6\text{O}_3$ ($\text{M} + \text{H}$) $^+$ 479.2195, found 479.2212. Purity: 100%.

1-(4-((5-(3-(m-tolyloxy)azetidine-1-carbonyl)-7H-pyrrolo[2,3-d]pyrimidin-4-yl)amino)methyl)piperidin-1-yl)prop-2-en-1-one (21). Compound 21 was prepared from compound 49d. Yield: 46%. White solid. Mp: 117–118 °C. ^1H NMR (400 MHz, DMSO- d_6) δ 12.21 (s, 1H), 9.48 (t, $J = 5.7$ Hz, 1H), 8.08 (s, 1H), 7.61 (d, $J = 2.1$ Hz, 1H), 7.15 (t, $J = 7.8$ Hz, 1H), 6.81–6.71 (m, 2H), 6.68–6.58 (m, 2H), 6.02 (dd, $J = 16.7$, 2.5 Hz, 1H), 5.58 (dd, $J = 10.5$, 2.5 Hz, 1H), 5.04 (tt, $J = 6.7$, 3.8 Hz, 1H), 4.94–4.79 (m, 1H), 4.62–4.43 (m, 2H), 4.43–4.31 (m, 1H), 4.06–3.89 (m, 12H), 3.42–3.32 (m, 2H), 2.98 (t, $J = 12.8$ Hz, 1H), 2.57 (t, $J = 12.5$ Hz, 1H), 2.24 (s, 3H), 1.87–1.79 (m, 1H), 1.73 (t, $J = 11.2$ Hz, 2H), 1.14–0.98 (m, 2H). ^{13}C NMR (100 MHz, DMSO) δ 166.38, 164.59, 157.19, 156.81, 153.47, 151.08, 139.88, 129.99, 129.09, 127.34, 126.52, 122.61, 115.70, 112.10, 108.38, 101.48, 66.44, 45.50, 36.36, 30.97, 29.89, 21.57. HRMS (ESI): m/z calcd for $\text{C}_{26}\text{H}_{31}\text{N}_6\text{O}_3$ ($\text{M} + \text{H}$) $^+$ 475.2465, found 475.2458. Purity: 100%.

1-(4-((5-(3-(3-chlorophenoxy)azetidine-1-carbonyl)-7H-pyrrolo[2,3-d]pyrimidin-4-yl)amino)methyl)piperidin-1-yl)prop-2-en-1-one (22). Compound 22 was prepared from compound 49e. Yield: 44%. White solid. Mp: 120–121 °C. ^1H NMR (400 MHz, DMSO- d_6) δ 12.27 (s, 1H), 9.52 (t, $J = 5.7$ Hz, 1H), 8.14 (s, 1H), 7.67 (s, 1H), 7.35 (t, $J = 8.2$ Hz, 1H), 7.12–7.02 (m, 1H), 6.97 (t, $J = 2.2$ Hz, 1H), 6.92–6.83 (m, 1H), 6.80 (dd, $J = 16.7$, 10.5 Hz, 1H), 6.07 (dd, $J = 16.7$, 2.5 Hz, 1H), 5.63 (dd, $J = 10.4$, 2.5 Hz, 1H), 5.22–5.11 (m, 1H), 5.00–4.83 (m, 1H), 4.63–4.48 (m, 2H), 4.48–4.36 (m, 1H), 4.12–3.91 (m, 2H), 3.48–3.37 (m, 2H), 3.02 (t, $J = 13.1$ Hz, 1H), 2.62 (t, $J = 12.6$ Hz, 1H), 1.94–1.83 (m, 1H), 1.85–1.68 (m, 2H), 1.19–0.97 (m, 2H). ^{13}C NMR (100 MHz, DMSO) δ 166.42, 164.59, 157.76, 157.18, 153.48, 151.10, 134.48, 131.70, 129.09, 127.34, 126.58, 121.93, 115.21, 114.26, 108.32, 101.46, 66.99, 45.50, 36.36, 30.97, 29.89. HRMS (ESI): m/z calcd for $\text{C}_{25}\text{H}_{28}\text{ClN}_6\text{O}_3$ ($\text{M} + \text{H}$) $^+$ 495.1891, found 495.1892. Purity: 100%.

1-(4-((5-(3-(trifluoromethyl)phenoxy)azetidine-1-carbonyl)-7H-pyrrolo[2,3-d]pyrimidin-4-yl)amino)methyl)piperidin-1-yl)prop-2-en-1-one (23). Compound 23 was prepared from compound 49f. Yield: 39%. White solid. Mp: 108–110 °C. ^1H NMR (400 MHz, DMSO- d_6) δ 12.22 (s, 1H), 9.47 (t, $J = 5.5$ Hz, 1H), 8.09 (s, 1H), 7.63 (d, $J = 2.6$ Hz, 1H), 7.53 (t, $J = 7.9$ Hz, 1H), 7.32 (d, $J = 7.7$ Hz, 1H), 7.21–7.03 (m, 2H), 6.75 (dd, $J = 16.7$, 10.5 Hz, 1H), 6.02 (dd, $J = 16.7$, 2.5 Hz, 1H), 5.59 (dd, $J = 10.4$, 2.5 Hz, 1H), 5.20 (tt, $J = 6.8$, 3.9 Hz, 1H), 4.98–4.82 (m, 1H), 4.65–4.47 (m, 2H), 4.44–4.32 (m, 1H), 4.08–3.91 (m, 2H), 3.48–3.30 (m, 2H), 2.98 (t, $J = 12.9$ Hz, 1H), 2.57 (t, $J = 12.7$ Hz, 1H), 1.84–1.80 (m, 1H), 1.74 (t, $J = 11.1$ Hz, 2H), 1.16–1.00 (m, 2H). ^{13}C NMR (100 MHz, DMSO) δ 166.45, 164.59,

157.18, 157.14, 153.48, 151.10, 131.58, 131.23, 130.91, 129.09, 127.33, 126.59, 125.71, 123.00, 119.30, 118.51, 111.94, 108.31, 101.46, 67.09, 45.50, 41.85, 36.36, 30.97, 29.89, 3.73. HRMS (ESI): m/z calcd for $C_{26}H_{28}F_3N_6O_3$ ($M + H$)⁺ 529.2178, found 529.2173. Purity: 100%.

1-(4-((5-(3-(naphthalen-1-yloxy)azetidine-1-carbonyl)-7*H*-pyrrolo[2,3-d]pyri midin-4-yl)amino)methyl)piperidin-1-ylprop-2-en-1-one (24). Compound **24** was prepared from compound **49g**. Yield: 39%. White solid. Mp: 128–130 °C. ¹H NMR (400 MHz, DMSO-*d*₆) δ 12.21 (s, 1H), 9.55–9.37 (m, 1H), 8.23–8.14 (m, 1H), 8.08 (s, 1H), 7.89–7.78 (m, 1H), 7.63 (s, 1H), 7.47 (d, $J = 7.9$ Hz, 3H), 7.35 (t, $J = 8.1$ Hz, 1H), 6.78–6.63 (m, 2H), 6.05–5.93 (m, 1H), 5.62–5.44 (m, 1H), 5.34–5.20 (m, 1H), 5.01–4.81 (m, 1H), 4.77–4.52 (m, 2H), 4.45–4.31 (m, 1H), 4.20–3.88 (m, 2H), 3.43–3.30 (m, 2H), 2.95 (t, $J = 12.9$ Hz, 1H), 2.55 (t, $J = 13.9$ Hz, 1H), 1.86–1.75 (m, 1H), 1.76–1.63 (m, 2H), 1.14–0.95 (m, 2H).

¹³C NMR (100 MHz, DMSO) δ 166.45, 164.59, 157.20, 153.47, 152.20, 151.09, 134.67, 129.08, 128.03, 127.34, 127.17, 126.56, 126.06, 125.20, 121.99, 121.32, 108.42, 106.10, 101.50, 66.96, 45.51, 41.86, 36.37, 30.98, 29.90. HRMS (ESI): m/z calcd for $C_{29}H_{31}N_6O_3$ ($M + H$)⁺

511.2466, found 511.2468. Purity: 100%.

1-(4-((5-(3-(naphthalen-2-yloxy)azetidine-1-carbonyl)-7*H*-pyrrolo[2,3-d]pyri midin-4-yl)amino)methyl)piperidin-1-ylprop-2-en-1-one (25). Compound **25** was prepared from compound **49h**. Yield: 42%. White solid. Mp: 121–122 °C. ¹H NMR (400 MHz, DMSO-*d*₆) δ 12.28 (s, 1H), 9.55 (t, $J = 6.0$ Hz, 1H), 8.15 (s, 1H), 7.96–7.80 (m, 3H), 7.69 (s, 1H), 7.49 (t, $J = 7.6$ Hz, 1H), 7.38 (t, $J = 7.5$ Hz, 1H), 7.25–7.04 (m, 2H), 6.79 (dd, $J = 16.7, 10.4$ Hz, 1H), 6.07 (d, $J = 16.6$ Hz, 1H), 5.63 (d, $J = 10.5$ Hz, 1H), 5.33–5.17 (m, 1H), 5.09–4.93 (m, 1H), 4.75–4.58 (m, 2H), 4.50–4.32 (m, 1H), 4.18–3.92 (m, 2H), 3.49–3.36 (m, 2H), 3.03 (t, $J = 12.3$ Hz, 1H), 2.62 (t, $J = 12.7$ Hz, 1H), 1.92–1.69 (m, 3H), 1.25–0.93 (m, 2H). ¹³C NMR (100 MHz, DMSO) δ 166.43, 164.59, 157.21, 154.62, 153.49, 151.11, 134.60, 130.28, 129.29, 129.08, 128.04, 127.34, 127.27, 127.05, 126.54, 124.47, 118.89, 108.40, 107.76, 101.50, 66.79, 55.39, 45.51, 41.86, 36.37, 30.98, 29.90. HRMS (ESI): m/z calcd for $C_{29}H_{31}N_6O_3$ ($M + H$)⁺ 511.2472, found 511.2471. Purity: 100%.

1-(4-((5-(3-(pyridin-2-yloxy)azetidine-1-carbonyl)-7*H*-pyrrolo[2,3-d]pyrimidi n-4-yl)amino)methyl)piperidin-1-ylprop-2-en-1-one (26). Compound **26** was prepared from compound **49i**. Yield: 49%. White solid. Mp: 128–129 °C. ¹H NMR (400 MHz, DMSO-*d*₆) δ 12.24 (s, 1H), 9.55 (s, 1H), 8.15 (d, $J = 17.1$ Hz, 2H), 7.77 (s, 1H), 7.65 (s, 1H), 7.05 (s, 1H), 7.00–6.89 (m, 1H), 6.79 (s, 1H), 6.24–5.93 (m, 1H), 5.78–5.59 (m, 1H), 5.49–5.36 (m, 1H), 5.06–4.81 (m, 1H), 4.64–4.41 (m, 3H), 4.18–3.92 (m, 2H), 3.55–3.37 (m, 2H), 3.16–2.95 (m, 1H), 2.70–2.56 (m, 1H), 1.95–1.75 (m, 3H), 1.31–1.00 (m, 2H).

¹³C NMR (100 MHz, DMSO) δ 166.42, 164.59, 162.34, 157.20, 153.44, 151.06, 147.47, 140.13, 129.09, 127.33, 126.47, 118.31, 111.37, 108.46, 101.49, 65.50, 65.41, 45.48, 41.86, 36.37, 30.98, 30.47, 29.90, 19.12, 14.02. HRMS (ESI): m/z calcd for $C_{24}H_{28}N_7O_3$ ($M + H$)⁺

462.2263, found 462.2261. Purity: 96.1%.

1-(4-((5-(3-(benzyloxy)azetidine-1-carbonyl)-7*H*-pyrrolo[2,3-d]pyrimidin-4-yl) amino)methyl)piperidin-1-ylprop-2-en-1-one (27). Compound **27** was prepared from compound **49j**. Yield: 36%. White solid. Mp: 87–89 °C. ¹H NMR (400 MHz, DMSO-*d*₆) δ 12.19 (s, 1H), 9.53 (t, $J = 5.7$ Hz, 1H), 8.08 (s, 1H), 7.55 (s, 1H), 7.35–7.22 (m, 5H), 6.73 (dd, $J = 16.8, 10.5$ Hz, 1H), 6.02 (dd, $J = 16.7, 2.5$ Hz, 1H), 5.58 (dd, $J = 10.4, 2.5$ Hz, 1H), 4.68–4.55 (m, 1H), 4.48–4.29 (m, 5H), 4.30–4.16 (m, 1H), 4.05–3.94 (m, 1H), 3.90–3.77 (m, 1H), 3.42–3.29 (m, 2H), 2.96 (t, $J = 12.8$ Hz, 1H), 2.56 (t, $J = 12.5$ Hz, 1H), 1.87–1.77 (m, 1H), 1.78–1.64 (m, 2H), 1.14–0.95 (m, 2H). ¹³C NMR (100 MHz, DMSO) δ 166.29, 164.58, 157.20, 153.45, 151.02, 138.04, 129.08, 128.80, 128.50, 128.22, 127.33, 126.22, 108.60, 101.49, 70.45, 68.00, 45.49, 41.85, 36.36, 30.97, 29.90. HRMS (ESI): m/z calcd for

$C_{26}H_{31}N_6O_3$ ($M + H$)⁺ 475.2463, found 475.2463. Purity: 100%.

1-(4-((5-(3-isopropoxyazetidine-1-carbonyl)-7*H*-pyrrolo[2,3-d]pyrimidin-4-yl) amino)methyl)piperidin-1-ylprop-2-en-1-one (28). Compound **28** was prepared from compound **49k**. Yield: 40%. White solid. Mp: 175–178 °C. ¹H NMR (400 MHz, DMSO-*d*₆) δ 12.22 (s, 1H), 9.59 (t, $J = 5.7$ Hz, 1H), 8.12 (s, 1H), 7.59 (s, 1H), 6.79 (dd, $J = 16.7, 10.5$ Hz, 1H), 6.07 (dd, $J = 16.7, 2.5$ Hz, 1H), 5.63 (dd, $J = 10.5, 2.5$ Hz, 1H), 4.65 (s, 1H), 4.50–4.38 (m, 2H), 4.32 (s, 2H), 4.06 (d, $J = 13.6$ Hz, 1H), 3.82 (s, 1H), 3.64 (hept, $J = 6.1$ Hz, 1H), 3.49–3.34 (m, 2H), 3.02 (t, $J = 12.8$ Hz, 1H), 2.62 (t, $J = 12.5$ Hz, 1H), 1.92–1.82 (m, 1H), 1.83–1.70 (m, 2H), 1.11 (d, $J = 6.1$ Hz, 8H). ¹³C NMR (100 MHz, DMSO) δ 166.15, 164.58, 157.21, 153.43, 151.01, 129.09, 127.32, 126.24, 108.63, 101.49, 70.87, 66.08, 45.48, 41.85, 36.36, 30.97, 29.89, 22.72, 22.53. HRMS (ESI): m/z calcd for $C_{22}H_{31}N_6O_3$ ($M + H$)⁺ 427.2443, found 427.2445. Purity: 100%.

4.2.2. General synthetic procedure for compounds **2, 29–45**

To a solution of compound **59 a-j, 61 a-f and 66 a-b** (1.0 eq) in DCM was added trifluoroacetic acid (70 eq) dropwise. The mixture was stirred at room temperature for 7h and then added saturated NaOH solution to adjust the pH to 12 and stirred at room temperature for 0.5h. After quenching with water and extracted with ethyl acetate (3 \times), the organic phase was separated and washed with brine, dried over Na_2SO_4 , filtered, and concentrated in vacuo. The residue was purified by silica column chromatography (DCM/MeOH) to afford the desired products compounds **2, 29–45**.

N-(4-(5-(1-acryloyl-1,2,3,6-tetrahydropyridin-4-yl)-7*H*-pyrrolo[2,3-d]pyrimidi n-4-yl)-2-methylbenzyl)-4-(tert-butyl)benzamide (2). Compound **2** was prepared from compound **59a**. Yield: 73%. White solid. Mp: 165–166 °C. ¹H NMR (400 MHz, DMSO-*d*₆) δ 12.20 (s, 1H), 8.91–8.78 (m, 1H), 8.74 (s, 1H), 7.79 (d, $J = 8.0$ Hz, 2H), 7.55–7.44 (m, 1H), 7.46–7.38 (m, 3H), 7.35 (s, 1H), 7.33–7.25 (m, 1H), 6.74–6.57 (m, 1H), 6.06 (t, $J = 16.2$ Hz, 1H), 5.60 (t, $J = 9.4$ Hz, 1H), 5.40–5.10 (m, 1H), 4.46 (d, $J = 5.7$ Hz, 2H), 3.85 (s, 2H), 3.39–3.31 (m, 1H), 3.19–3.08 (m, 1H), 2.30 (s, 3H), 1.96–1.82 (m, 2H), 1.24 (s, 9H). ¹³C NMR (100 MHz, DMSO) δ 166.12, 164.21, 158.11, 153.98, 152.51, 150.73, 138.67, 136.76, 134.99, 131.60, 131.07, 129.94, 128.59, 128.31, 127.39, 127.12, 126.32, 125.07, 122.78, 122.38, 116.33, 112.78, 44.45, 41.87, 40.51, 34.59, 30.94, 30.74, 22.09, 18.78. HRMS (ESI): m/z calcd for $C_{33}H_{36}O_2N_5$ ($M + H$)⁺ 534.2864, found 534.2851. Purity: 100%.

N-(4-(5-(1-(but-2-ynoyl)-1,2,3,6-tetrahydropyridin-4-yl)-7*H*-pyrrolo[2,3-d]pyrimidi n-4-yl)-2-methylbenzyl)-4-(tert-butyl)benzamide (29). Compound **29** was prepared from compound **59b**. Yield: 85%. White solid. Mp: 162–163 °C. ¹H NMR (400 MHz, DMSO-*d*₆) δ 12.21 (s, 1H), 8.87–8.78 (m, 1H), 8.75 (s, 1H), 7.85–7.76 (m, 2H), 7.54–7.51 (m, 1H), 7.50–7.37 (m, 3H), 7.36–7.25 (m, 2H), 5.30–5.19 (m, 1H), 4.48 (d, $J = 5.6$ Hz, 2H), 4.03–3.92 (m, 1H), 3.81–3.74 (m, 1H), 3.45 (t, $J = 5.4$ Hz, 1H), 3.29 (t, $J = 5.5$ Hz, 1H), 2.32 (s, 3H), 1.93–1.84 (m, 5H), 1.26 (s, 9H). ¹³C NMR (100 MHz, DMSO) δ 166.17, 158.23, 154.08, 152.58, 152.19, 150.87, 138.80, 136.79, 135.01, 134.89, 131.65, 131.41, 131.11, 130.12, 129.88, 127.21, 126.99, 126.47, 125.16, 122.09, 116.26, 112.84, 88.79, 72.97, 45.79, 43.11, 41.12, 34.68, 31.03, 30.43, 18.88, 3.45. HRMS (ESI): m/z calcd for $C_{34}H_{36}O_2N_5$ ($M + H$)⁺ 546.2864, found 546.2854. Purity: 100%.

N-(4-(5-(1-acryloyl-1,2,3,6-tetrahydropyridin-4-yl)-7*H*-pyrrolo[2,3-d]pyrimidi n-4-yl)-2-fluorobenzyl)-4-(tert-butyl)benzamide (30). Compound **30** was prepared from compound **59c**. Yield: 81%. White solid. Mp: 179–180 °C. ¹H NMR (400 MHz, DMSO-*d*₆) δ 12.39 (s, 1H), 9.16–9.01 (m, 1H), 8.82 (s, 1H), 7.85 (d, $J = 7.4$ Hz, 2H), 7.66–7.54 (m, 1H), 7.51–7.34 (m, 5H), 6.69 (dd, $J = 16.6, 10.5$ Hz, 1H), 6.21–5.99 (m, 1H), 5.65 (t, $J = 10.2$ Hz, 1H), 5.41–5.10 (m, 1H), 4.57 (d, $J = 5.4$ Hz, 2H), 3.94–3.84 (m, 2H), 3.45 (t, $J = 4.5$ Hz, 1H), 3.41–3.34 (m, 1H), 2.06–1.98 (m, 1H), 1.98–1.90 (m, 1H), 1.29 (s, 9H). ¹³C NMR (100 MHz, DMSO) δ 166.27, 164.25, 156.50, 154.08, 152.54, 150.72, 138.94, 134.27, 131.37, 129.69, 129.11, 128.87, 128.59, 128.30, 127.15, 127.06, 125.54, 125.07, 123.25, 122.92, 115.99, 112.84, 44.42, 42.46,

41.86, 36.35, 34.60, 30.93, 30.77. HRMS (ESI): m/z calcd for $C_{32}H_{33}O_2N_5F$ ($M + H$)⁺ 538.2613, found 538.2612. Purity: 100%.

N-(4-(5-(1-(but-2-ynoyl)-1,2,3,6-tetrahydropyridin-4-yl)-7H-pyrrolo[2,3-d] pyri-midin-4-yl)-2-fluorobenzyl)-4-(tert-butyl)benzamide (31). Compound 31 was prepared from compound 59d. Yield: 69%. White solid. Mp: 161–162 °C. ¹H NMR (400 MHz, DMSO- d_6) δ 12.33 (s, 1H), 9.05–8.94 (m, 1H), 8.83 (s, 1H), 7.89–7.79 (m, 2H), 7.59 (d, J = 8.8 Hz, 1H), 7.52–7.42 (m, 3H), 7.46–7.34 (m, 2H), 5.30 (s, 1H), 4.59 (d, J = 5.7 Hz, 2H), 4.07–3.99 (m, 1H), 3.85–3.79 (m, 1H), 3.52 (t, J = 5.6 Hz, 1H), 3.38 (d, J = 6.8 Hz, 1H), 2.07–2.01 (m, 1H), 2.04–1.96 (m, 3H), 1.98–1.92 (m, 1H), 1.30 (s, 9H). ¹³C NMR (100 MHz, DMSO) δ 166.35, 166.29, 160.70, 158.27, 156.60, 156.52, 154.17, 152.61, 152.57, 152.14, 151.91, 150.81, 138.98, 138.90, 131.39, 131.36, 129.92, 129.68, 129.58, 128.98, 127.59, 127.44, 127.16, 127.14, 125.57, 125.28, 125.14, 122.59, 122.55, 115.95, 115.79, 115.56, 112.85, 112.68, 88.74, 72.90, 45.71, 43.04, 41.00, 37.51, 36.47, 34.64, 30.96, 30.39, 3.39. HRMS (ESI): m/z calcd for $C_{33}H_{33}O_2N_5F$ ($M + H$)⁺ 550.2613, found 550.2653. Purity: 100%.

N-(4-(5-(1-acryloyl-1,2,3,6-tetrahydropyridin-4-yl)-7H-pyrrolo[2,3-d] pyrimidi-n-4-yl)benzyl)-4-(tert-butyl)benzamide (32). Compound 32 was prepared from compound 59e. Yield: 69%. White solid. Mp: 132–133 °C. ¹H NMR (500 MHz, DMSO- d_6) δ 12.26 (s, 1H), 9.04–8.97 (m, 1H), 8.80 (s, 1H), 7.83 (d, J = 8.3 Hz, 2H), 7.61–7.51 (m, 3H), 7.50–7.44 (m, 2H), 7.40 (t, J = 9.4 Hz, 2H), 6.75–6.62 (m, 1H), 6.17–6.05 (m, 1H), 5.71–5.60 (m, 1H), 5.40–5.11 (m, 1H), 4.57–4.52 (m, 2H), 3.93–3.86 (m, 2H), 3.45–3.40 (m, 1H), 3.33 (t, J = 5.2 Hz, 1H), 2.02–1.95 (m, 1H), 1.92–1.85 (m, 1H), 1.30 (s, 9H). ¹³C NMR (100 MHz, DMSO) δ 166.24, 164.30, 158.11, 154.08, 152.60, 150.86, 141.15, 136.97, 131.69, 129.95, 129.41, 129.21, 128.75, 128.40, 127.35, 127.15, 127.14, 126.92, 126.68, 125.17, 123.06, 122.82, 116.34, 112.96, 44.53, 42.56, 41.95, 34.68, 31.02, 30.82. HRMS (ESI): m/z calcd for $C_{32}H_{34}O_2N_5$ ($M + H$)⁺ 520.2707, found 520.2744. Purity: 98.4%.

N-(4-(5-(1-(but-2-ynoyl)-1,2,3,6-tetrahydropyridin-4-yl)-7H-pyrrolo[2,3-d] pyri-midin-4-yl)benzyl)-4-(tert-butyl)benzamide (33). Compound 33 was prepared from compound 59f. Yield: 88%. White solid. Mp: 139–140 °C. ¹H NMR (400 MHz, DMSO- d_6) δ 12.27 (s, 1H), 9.04–8.94 (m, 1H), 8.81 (s, 1H), 7.86–7.81 (m, 2H), 7.61–7.57 (m, 2H), 7.55 (dd, J = 7.3, 2.4 Hz, 1H), 7.52–7.44 (m, 2H), 7.47–7.38 (m, 2H), 5.31 (d, J = 3.2 Hz, 1H), 4.56 (d, J = 5.9 Hz, 2H), 4.08–3.99 (m, 1H), 3.85–3.78 (m, 1H), 3.48 (t, J = 5.6 Hz, 1H), 3.32 (s, 1H), 2.04 (s, 1H), 1.98 (s, 3H), 1.98–1.86 (m, 1H), 1.30 (s, 9H). ¹³C NMR (100 MHz, DMSO) δ 166.12, 158.05, 154.00, 152.47, 152.08, 151.82, 150.79, 141.10, 136.78, 131.53, 130.07, 129.71, 129.22, 129.12, 127.05, 126.70, 125.07, 122.18, 116.11, 112.82, 88.65, 72.87, 45.68, 42.99, 42.42, 40.95, 37.47, 34.58, 30.92, 30.40, 30.31, 3.33. HRMS (ESI): m/z calcd for $C_{33}H_{34}O_2N_5$ ($M + H$)⁺ 532.2707, found 532.2696. Purity: 100%.

N-(4-(5-(1-acryloylpiperidin-4-yl)-7H-pyrrolo[2,3-d] pyrimidi-n-4-yl)-2-methylb-enzyl)-4-(tert-butyl)benzamide (34). Compound 34 was prepared from compound 61a. Yield: 50%. White solid. Mp: 164–165 °C. ¹H NMR (500 MHz, DMSO- d_6) δ 12.01 (s, 1H), 8.93 (s, 1H), 8.74 (s, 1H), 7.83 (d, J = 6.6 Hz, 2H), 7.53–7.37 (m, 5H), 7.34 (s, 1H), 6.70–6.59 (m, 1H), 6.02 (d, J = 17.0 Hz, 1H), 5.59 (d, J = 9.0 Hz, 1H), 4.65–4.49 (m, 2H), 4.37 (d, J = 11.4 Hz, 1H), 3.86 (d, J = 11.2 Hz, 1H), 2.73–2.64 (m, 1H), 2.64–2.54 (m, 1H), 2.46 (s, 3H), 2.28–2.14 (m, 1H), 1.61–1.52 (m, 1H), 1.49–1.38 (m, 1H), 1.29 (s, 9H), 1.26–1.18 (m, 2H). ¹³C NMR (100 MHz, DMSO) δ 166.22, 163.99, 158.84, 154.07, 152.22, 150.45, 138.56, 137.78, 135.29, 131.73, 130.25, 128.59, 127.29, 127.19, 126.90, 126.14, 125.16, 122.93, 118.55, 114.14, 45.63, 42.05, 40.57, 34.68, 33.88, 33.82, 32.40, 31.03, 18.80. HRMS (ESI): m/z calcd for $C_{33}H_{38}O_2N_5$ ($M + H$)⁺ 536.3020, found 536.3011. Purity: 99.2%.

N-(4-(5-(1-(but-2-ynoyl)piperidin-4-yl)-7H-pyrrolo[2,3-d] pyrimidi-n-4-yl)-2-me-thylbenzyl)-4-(tert-butyl)benzamide (35). Compound 35 was prepared from compound 61b. Yield: 64%. White solid. Mp: 162–163 °C. ¹H NMR (500 MHz, DMSO- d_6) δ 12.01 (s, 1H),

8.94–8.89 (m, 1H), 8.74 (s, 1H), 7.83 (d, J = 7.9 Hz, 2H), 7.47 (d, J = 7.7 Hz, 2H), 7.44–7.41 (m, 3H), 7.36 (s, 1H), 4.55 (d, J = 4.3 Hz, 2H), 4.22 (d, J = 12.9 Hz, 1H), 4.11 (d, J = 12.5 Hz, 1H), 2.65 (t, J = 11.9 Hz, 2H), 2.46 (s, 3H), 2.21 (t, J = 12.5 Hz, 1H), 1.97 (s, 3H), 1.60–1.49 (m, 2H), 1.30 (s, 9H), 1.26–1.24 (m, 2H). ¹³C NMR (100 MHz, DMSO) δ 166.18, 158.82, 154.07, 152.17, 151.67, 150.45, 138.57, 137.69, 135.27, 131.69, 130.19, 127.17, 126.11, 125.14, 123.02, 118.38, 114.09, 89.03, 73.13, 46.86, 41.11, 40.55, 34.68, 33.74, 33.38, 32.34, 31.02, 18.78, 3.41. HRMS (ESI): m/z calcd for $C_{34}H_{38}O_2N_5$ ($M + H$)⁺ 548.3020, found 548.3016. Purity: 96.3%.

N-(4-(5-(1-acryloylpiperidin-4-yl)-7H-pyrrolo[2,3-d] pyrimidi-n-4-yl)-2-fluorobenzo-nyl)-4-(tert-butyl)benzamide (36). Compound 36 was prepared from compound 61c. Yield: 71%. White solid. Mp: 154–155 °C. ¹H NMR (500 MHz, DMSO- d_6) δ 12.05 (s, 1H), 9.02 (t, J = 5.7 Hz, 1H), 8.73 (s, 1H), 7.79 (d, J = 8.1 Hz, 2H), 7.51 (t, J = 7.7 Hz, 1H), 7.45–7.33 (m, 5H), 6.62 (dd, J = 16.9, 10.4 Hz, 1H), 6.00 (d, J = 15.0 Hz, 1H), 5.56 (d, J = 12.0 Hz, 1H), 4.57 (d, J = 5.8 Hz, 2H), 4.34 (d, J = 13.0 Hz, 1H), 3.83 (d, J = 10.6 Hz, 1H), 2.63–2.53 (m, 2H), 2.21 (s, 1H), 1.55 (d, J = 12.6 Hz, 1H), 1.43 (d, J = 11.9 Hz, 1H), 1.26 (s, 9H), 1.23–1.20 (m, 2H). ¹³C NMR (100 MHz, DMSO) δ 166.32, 163.98, 160.82, 158.38, 157.22, 154.19, 152.30, 150.42, 140.02, 139.94, 131.46, 129.38, 128.57, 127.45, 127.30, 127.16, 126.89, 125.16, 124.85, 123.33, 118.36, 115.41, 115.19, 114.10, 56.10, 45.52, 41.94, 36.48, 34.68, 33.77, 32.27, 31.00. HRMS (ESI): m/z calcd for $C_{32}H_{35}O_2N_5F$ ($M + H$)⁺ 540.2769, found 540.2809. Purity: 100%.

N-(4-(5-(1-(but-2-ynoyl)piperidin-4-yl)-7H-pyrrolo[2,3-d] pyrimidi-n-4-yl)-2-fluoro-2-oro-benzyl)-4-(tert-butyl)benzamide (37). Compound 37 was prepared from compound 61d. Yield: 79%. White solid. Mp: 156–157 °C. ¹H NMR (400 MHz, DMSO- d_6) δ 12.12 (s, 1H), 9.08 (t, J = 5.9 Hz, 1H), 8.77 (s, 1H), 7.82 (d, J = 8.5 Hz, 2H), 7.57–7.50 (m, 1H), 7.49–7.45 (m, 3H), 7.43–7.38 (m, 2H), 4.60 (d, J = 5.7 Hz, 2H), 4.23 (d, J = 13.4 Hz, 1H), 4.11 (d, J = 15.8 Hz, 1H), 2.71–2.57 (m, 2H), 2.26–2.23 (m, 1H), 1.98 (s, 3H), 1.54 (d, J = 12.4 Hz, 2H), 1.30 (s, 9H), 1.24 (s, 2H). ¹³C NMR (100 MHz, DMSO) δ 166.21, 160.71, 158.27, 157.12, 154.11, 152.16, 151.57, 150.32, 131.33, 129.26, 127.05, 125.06, 124.76, 123.31, 118.10, 113.97, 88.91, 73.01, 46.67, 42.24, 40.90, 36.39, 34.58, 33.55, 33.28, 32.11, 30.90, 3.30. HRMS (ESI): m/z calcd for $C_{33}H_{35}O_2N_5F$ ($M + H$)⁺ 552.2769, found 552.2811. Purity: 100%.

N-(4-(5-(1-acryloylpiperidin-4-yl)-7H-pyrrolo[2,3-d] pyrimidi-n-4-yl)benzyl)-4-(tert-butyl)benzamide (38). Compound 38 was prepared from compound 61e. Yield: 71%. White solid. Mp: 152–153 °C. ¹H NMR (400 MHz, DMSO- d_6) δ 11.98 (s, 1H), 9.02 (t, J = 6.0 Hz, 1H), 8.70 (s, 1H), 7.77 (d, J = 8.5 Hz, 2H), 7.52 (d, J = 8.1 Hz, 2H), 7.49–7.37 (m, 4H), 7.30 (d, J = 2.1 Hz, 1H), 6.59 (dd, J = 16.7, 10.5 Hz, 1H), 5.97 (dd, J = 16.7, 2.4 Hz, 1H), 5.54 (dd, J = 10.5, 2.4 Hz, 1H), 4.52 (d, J = 5.9 Hz, 2H), 4.29 (d, J = 12.6 Hz, 1H), 3.78 (d, J = 14.6 Hz, 1H), 2.68–2.51 (m, 2H), 2.21–2.12 (m, 1H), 1.51 (d, J = 13.9 Hz, 1H), 1.38 (d, J = 13.2 Hz, 1H), 1.24 (s, 9H), 1.22–1.20 (m, 2H). ¹³C NMR (100 MHz, DMSO) δ 166.21, 163.96, 158.77, 154.08, 152.24, 150.46, 141.00, 137.85, 131.70, 128.71, 128.58, 127.11, 127.01, 126.85, 125.15, 122.89, 118.50, 114.16, 45.51, 42.58, 41.93, 34.67, 33.76, 33.70, 32.24, 31.01. HRMS (ESI): m/z calcd for $C_{32}H_{36}O_2N_5$ ($M + H$)⁺ 522.2864, found 522.2905. Purity: 100%.

N-(4-(5-(1-(but-2-ynoyl)piperidin-4-yl)-7H-pyrrolo[2,3-d] pyrimidi-n-4-yl)-2-tert-butylbenzyl)-4-(tert-butyl)benzamide (39). Compound 39 was prepared from compound 61f. Yield: 71%. White solid. Mp: 156–157 °C. ¹H NMR (400 MHz, DMSO- d_6) δ 12.06 (s, 1H), 9.07 (t, J = 6.0 Hz, 1H), 8.76 (s, 1H), 7.82 (d, J = 8.4 Hz, 2H), 7.57 (d, J = 7.9 Hz, 2H), 7.54–7.43 (m, 4H), 7.37 (s, 1H), 4.57 (d, J = 6.0 Hz, 2H), 4.20 (d, J = 13.5 Hz, 1H), 4.08 (d, J = 12.5 Hz, 1H), 2.67–2.60 (m, 2H), 2.26–2.16 (m, 1H), 1.97 (s, 3H), 1.51 (d, J = 12.0 Hz, 2H), 1.31 (s, 9H), 1.28–1.22 (m, 2H). ¹³C NMR (100 MHz, DMSO) δ 166.21, 158.71, 154.09, 152.21, 151.65, 150.41, 141.06, 137.69, 131.67, 128.69, 127.11, 127.00, 125.14, 123.02, 118.37, 114.14, 88.99, 73.11, 46.76, 42.59, 40.99, 34.67, 33.59, 33.31, 32.19, 31.01, 3.40. HRMS (ESI): m/z calcd for

$C_{33}H_{36}O_2N_5$ ($M + H$)⁺ 534.2864, found 534.2903. Purity: 99.1%. **N-(4-(5-(1-acryloyl-1,2,3,6-tetrahydropyridin-4-yl)-7H-pyrrolo[2,3-d]pyrimidi-n-4-yl)-2-fluorobenzyl)-4-cyclopropylbenzamide (40).** Compound **40** was prepared from compound **59g**. Yield: 69%. White solid. Mp: 135–136 °C. ¹H NMR (400 MHz, DMSO-*d*₆) δ 12.36 (s, 1H), 9.01–8.93 (m, 1H), 8.82 (s, 1H), 7.78 (d, *J* = 7.3 Hz, 2H), 7.66–7.54 (m, 1H), 7.48–7.31 (m, 3H), 7.19–7.06 (m, 2H), 6.68 (dd, *J* = 16.5, 10.6 Hz, 1H), 6.10 (dd, *J* = 17.1, 9.0 Hz, 1H), 5.66 (t, *J* = 8.1 Hz, 1H), 5.40–5.10 (m, 1H), 4.56 (d, *J* = 5.7 Hz, 2H), 3.94–3.83 (m, 2H), 3.45 (t, *J* = 4.4 Hz, 1H), 3.36 (t, *J* = 5.4 Hz, 1H), 2.07–1.99 (m, 1H), 2.00–1.90 (m, 2H), 1.07–0.95 (m, 2H), 0.78–0.68 (m, 2H). ¹³C NMR (100 MHz, DMSO) δ 166.17, 164.24, 164.04, 156.51, 152.56, 150.73, 147.66, 131.04, 129.68, 129.16, 128.55, 128.24, 127.27, 127.08, 125.49, 125.05, 123.29, 122.94, 116.03, 115.96, 115.76, 115.54, 112.84, 112.51, 44.42, 41.83, 38.01, 36.41, 30.76, 29.28, 15.09, 10.06. HRMS (ESI): *m/z* calcd for $C_{31}H_{29}O_2N_5F$ ($M + H$)⁺ 522.2300, found 522.2291. Purity: 98.9%.

N-(4-(5-(1-(but-2-ynoyl)-1,2,3,6-tetrahydropyridin-4-yl)-7H-pyrrolo[2,3-d]pyrimidin-4-yl)-2-fluorobenzyl)-4-cyclopropylbenzamide (41). Compound **41** was prepared from compound **59h**. Yield: 80%. White solid. Mp: 135–136 °C. ¹H NMR (400 MHz, DMSO-*d*₆) δ 12.29 (s, 1H), 8.96–8.87 (m, 1H), 8.78 (s, 1H), 7.80–7.69 (m, 2H), 7.55 (dd, *J* = 10.2, 2.4 Hz, 1H), 7.45–7.29 (m, 3H), 7.10 (d, *J* = 8.4 Hz, 2H), 5.31–5.14 (m, 1H), 4.52 (d, *J* = 5.4 Hz, 2H), 4.04–3.93 (m, 1H), 3.80–3.71 (m, 1H), 3.46 (t, *J* = 5.8 Hz, 1H), 3.32 (t, *J* = 5.9 Hz, 1H), 1.99–1.88 (m, 6H), 1.00–0.91 (m, 2H), 0.73–0.63 (m, 2H). ¹³C NMR (100 MHz, DMSO) δ 166.19, 166.15, 158.21, 156.48, 152.54, 152.51, 152.08, 151.86, 150.75, 147.65, 138.94, 138.87, 131.02, 131.00, 129.84, 129.57, 128.99, 127.58, 127.30, 125.54, 125.21, 125.04, 122.46, 115.88, 112.80, 112.62, 89.73, 88.72, 73.17, 72.84, 45.65, 42.96, 40.94, 37.45, 36.38, 30.35, 29.27, 15.10, 10.06, 3.33. HRMS (ESI): *m/z* calcd for $C_{32}H_{29}O_2N_5F$ ($M + H$)⁺ 534.2300, found 534.2294. Purity: 97.7%.

N-(4-(5-(1-acryloyl-1,2,3,6-tetrahydropyridin-4-yl)-7H-pyrrolo[2,3-d]pyrimidi-n-4-yl)-2-fluorobenzyl)benzamide (42). Compound **42** was prepared from compound **59i**. Yield: 59%. White solid. Mp: 159–160 °C. ¹H NMR (500 MHz, DMSO-*d*₆) δ 12.31 (s, 1H), 9.10–9.03 (m, 1H), 8.83 (s, 1H), 7.90 (d, *J* = 6.5 Hz, 2H), 7.63–7.50 (m, 2H), 7.50–7.36 (m, 5H), 6.73–6.64 (m, 1H), 6.15–6.06 (m, 1H), 5.69–5.61 (m, 1H), 5.40–5.14 (m, 1H), 4.58 (d, *J* = 5.7 Hz, 2H), 3.94–3.87 (m, 2H), 3.49–3.43 (m, 1H), 3.41–3.35 (m, 1H), 2.06–1.99 (m, 1H), 2.01–1.95 (m, 1H).

¹³C NMR (100 MHz, DMSO) δ 166.38, 164.26, 164.05, 156.50, 152.56, 150.74, 134.11, 131.33, 129.66, 128.55, 128.32, 127.24, 125.50, 123.30, 122.94, 116.02, 112.83, 44.42, 41.83, 38.01, 36.51, 30.75, 29.28. HRMS (ESI): *m/z* calcd for $C_{28}H_{25}O_2N_5F$ ($M + H$)⁺ 482.1987, found 482.2025. Purity: 100%.

N-(4-(5-(1-(but-2-ynoyl)-1,2,3,6-tetrahydropyridin-4-yl)-7H-pyrrolo[2,3-d]pyrimidin-4-yl)-2-fluorobenzyl)benzamide (43). Compound **43** was prepared from compound **59j**. Yield: 60%. White solid. Mp: 146–147 °C. ¹H NMR (500 MHz, DMSO-*d*₆) δ 12.33 (s, 1H), 9.09–9.01 (m, 1H), 8.83 (s, 1H), 7.90 (t, *J* = 6.8 Hz, 2H), 7.62–7.52 (m, 2H), 7.50–7.37 (m, 5H), 5.36–5.27 (m, 1H), 4.60 (d, *J* = 5.9 Hz, 2H), 4.08–4.02 (m, 1H), 3.86–3.80 (m, 1H), 3.53 (t, *J* = 5.7 Hz, 1H), 3.38 (t, *J* = 5.3 Hz, 1H), 2.06–1.95 (m, 5H). ¹³C NMR (100 MHz, DMSO) δ 166.50, 166.45, 156.63, 152.66, 152.63, 152.18, 151.97, 150.86, 134.20, 134.17, 131.43, 129.93, 129.67, 129.17, 128.42, 127.36, 127.34, 125.64, 125.33, 122.67, 122.57, 116.00, 115.65, 112.91, 112.72, 89.85, 88.84, 73.26, 72.93, 56.10, 45.75, 43.06, 41.04, 37.54, 36.61, 31.04, 30.45, 29.36, 22.15, 18.64, 14.05, 3.46, 3.43. HRMS (ESI): *m/z* calcd for $C_{29}H_{25}O_2N_5F$ ($M + H$)⁺ 494.1987, found 494.2023. Purity: 97.0%.

1-(4-(5-(1-acryloyl-1,2,3,6-tetrahydropyridin-4-yl)-7H-pyrrolo[2,3-d]pyrimidin-4-yl)-2-fluorobenzyl)-3-phenylurea (44). Compound **44** was prepared from compound **66a**. Yield: 50%. White solid. Mp: 187–188 °C.

¹H NMR (400 MHz, DMSO-*d*₆) δ 12.32 (s, 1H), 8.78 (s, 1H), 8.63 (s,

1H), 7.61–7.51 (m, 1H), 7.44–7.29 (m, 5H), 7.15 (t, *J* = 7.8 Hz, 2H), 6.84 (t, *J* = 7.3 Hz, 1H), 6.70–6.53 (m, 2H), 6.13–6.00 (m, 1H), 5.72–5.50 (m, 1H), 5.35–5.21 (m, 1H), 4.36 (d, *J* = 5.7 Hz, 2H), 3.90–3.82 (m, 2H), 3.47–3.33 (m, 2H), 2.06–1.97 (m, 1H), 1.96–1.86 (m, 1H).

¹³C NMR (100 MHz, DMSO) δ 164.31, 164.06, 156.47, 155.14, 152.59, 150.73, 140.33, 129.72, 129.64, 128.63, 128.24, 127.21, 127.12, 125.56, 125.33, 125.13, 123.25, 122.99, 121.14, 117.66, 116.01, 115.94, 115.83, 112.79, 112.47, 44.46, 41.87, 38.02, 36.76, 30.74, 29.28. HRMS (ESI): *m/z* calcd for $C_{28}H_{26}O_2N_6F$ ($M + H$)⁺ 497.2096, found 497.2087. Purity: 98.3%.

1-(4-(5-(1-(but-2-ynoyl)-1,2,3,6-tetrahydropyridin-4-yl)-7H-pyrrolo[2,3-d]pyrimidin-4-yl)-2-fluorobenzyl)-3-phenylurea (45). Compound **45** was prepared from compound **66b**. Yield: 61%. White solid. Mp: 156–157 °C.

¹H NMR (400 MHz, DMSO-*d*₆) δ 12.38 (s, 1H), 9.08–8.94 (m, 1H), 8.83 (s, 1H), 7.60 (dd, *J* = 13.9, 2.4 Hz, 1H), 7.56–7.41 (m, 2H), 7.40 (d, *J* = 7.6 Hz, 3H), 7.20 (t, *J* = 7.9 Hz, 2H), 7.00–6.93 (m, 1H), 6.88 (t, *J* = 7.3 Hz, 1H), 5.35–5.25 (m, 1H), 4.42 (d, *J* = 5.5 Hz, 2H), 4.08–3.97 (m, 1H), 3.90–3.82 (m, 1H), 3.60–3.54 (m, 1H), 3.46–3.38 (m, 1H), 1.99–1.96 (m, 5H).

¹³C NMR (100 MHz, DMSO) δ 160.66, 155.25, 155.22, 152.56, 152.10, 151.85, 150.75, 140.41, 140.39, 129.80, 129.66, 128.61, 125.60, 122.59, 122.44, 121.06, 117.61, 117.59, 115.89, 112.75, 112.56, 89.69, 88.74, 72.85, 45.67, 42.97, 40.96, 37.46, 36.69, 30.34, 29.26, 3.29. HRMS (ESI): *m/z* calcd for $C_{29}H_{26}O_2N_6F$ ($M + H$)⁺ 509.2096, found 509.2089. Purity: 100%.

4.3. BTK enzymatic assay

ADP-Glo™ assay kits from Promega Corporation were used according to instructions. 11 concentrations were used (10 μM–1 nM) for ATP competition experiments. 50 μL compound was added to 384-well dilution plate and 0.05 μL diluted compound solution was transferred in each row to 384 assay plate using Echo and each column containing 2 replicates. 2.5 μL enzyme working solution was added to 384-well assay plate and incubate with compounds at 25 °C for 15 min. 2.5 μL substrate working solution was added to initiate reaction and 4 μL ADP Glo reagent was added after 60 min. 60 min later, 8 μL kinase detection reagent was added and incubate at 25 °C for 60 min. The luminescence signal was read with an envision Perkin Elmer plate reader (Envision, PE, USA).

4.4. In vitro anti-proliferation efficacy

Cell proliferation assay was performed with the CellTiter-Glo assay (Promega). The cells were inoculated in 96-well plates at a density of 3×10^3 cells/well, and the cells were treated with test compounds at 37 °C, 5% CO₂ for 72 h. Then 50 μL CellTiter-Glo Reagent was added into each well. Contents were mixed for 2 min on an orbital shaker to induce cell lysis. The plates incubated at room temperature for 10 min to stabilize luminescent signal. The luminescence was recorded on Envision. IC₅₀ values were calculated with GraphPad Prism 7.0 software.

4.5. Pharmacokinetic studies

Test compounds were subjected to pharmacokinetic studies on male BALB/c mice. For oral administration, nine animals were in each group and three animals were in each group for intravenous administration. The test compounds were orally administered as 0.5% CMC/water (10 mg/kg) or intravenous injected as 2.5% DMSO/20% hydroxypropyl-β-cyclodextrin (2 mg/kg). Blood samples were collected at 0.083, 0.167, 0.25, 0.5, 1, 2, 4, 6, 8, and 12 h time points following oral dosing and at 0.083, 0.167, 0.25, 0.5, 1, 2, 4, 6, 8, and 12 h following intravenous dosing.

4.6. Western Blot Analysis

Western Blot Analysis. TMD8 cells were pretreated with various concentrations of compound wj1113 for 2 h and stimulated with anti-IgM F(ab')2 (Jackson ImmunoResearch, West Grove, USA) for 10 min. After the cells were lysed with RIPA buffer (Sigma-Aldrich) on ice for 30 min, the proteins were separated by sodium dodecyl sulfate polyacrylamide gel electrophoresis (SDS-PAGE), and then transferred to poly(vinylidene fluoride) (PVDF) membranes. Membranes were incubated at 4 °C with primary antibodies specific for BTK, pBTK Y233, PLC γ 2, PLC γ 2 Y1217 (Cell Signaling Technologies) or GAPDH (TRANS) overnight. After being incubated with anti-rabbit horseradish peroxidase-conjugated secondary antibodies for 1 h, the specific bands were detected using a ECL kit.

4.7. Flow cytometry analysis of apoptotic cells

TMD8 cells were cultured in 12-well plates at a density of 4×10^5 per well and incubated with various concentrations of compounds **42**, or 0.1% (v/v) dimethyl sulfoxide (DMSO) at 37 °C in a humidified atmosphere containing 5% CO₂ for 72 h. The cells were washed with cold PBS, collected by centrifugation, and resuspended in 1 × binding buffer. Then, the Annexin-V-FITC dye was added to the treated cells and incubated for 15 min. The distribution of cell cycle phases was analyzed with flow cytometry (Beckman Coulter, Inc, Cytoflexs) after PI was added 5 min later.

4.8. Cell cycle analysis

TMD8 cells were treated with indicated concentrations of compounds **42** or 0.1% (v/v) DMSO for 48 h. After being washed with cold PBS and centrifuged. Then, the cells were dyed with 200 μL of PI for 30 min at 37 °C and analyzed by flow cytometry.

4.9. Antitumor activity of compound **42** in vivo

The experiment was carried out in compliance with institutional guidelines approved by AAALAC. For the subcutaneous mouse model, female CB-17 SCID mice (6–8 weeks old) were subcutaneously implanted with 1×10^7 cells of TMD8. When the average tumor volumes reached 150 mm³–200 mm³, the mice were randomized and administered by intragastric with compounds twice daily for 21 consecutive days. During treatment, tumor volume and body weight were monitored twice a week. Mice were sacrificed at the end of the treatment, and the tumors were removed. Tumor volume inhibition (TGI) was measured as (1-RTV treatment/RTV vehicle) × 100.

4.10. Molecular docking

The molecular docking was conducted with Covalent Docking in Glide in the Schrodinger software. Briefly, the crystal structure of BTK (PDB ID: 5P9J and PDB ID: 5VFI) was downloaded from the Protein Data Bank and prepared with the Protein Preparation Wizard. The Grid Generation tool was then employed to indicate the binding pocket in the protein. The docking was conducted with the Covalent Docking wizard between the prepared molecules and the target protein. The binding modes were analyzed with Pymol.

4.11. Workflow of hierarchical virtual screening

For commercially available compound libraries, 9994 compounds from the Drugbank database and 100000 compounds from Chemdiv were subjected to XGraphBoost and 184 compounds were retained with probability of being active higher than 0.5. In addition, molecular properties, such as molecule weight, clogP, of BTK inhibitors in Chembank had been calculated by RDKit and the range of these properties were

regarded as filters. Further, structures that do not have warheads were removed and 10 molecules were retained. For generated compounds, 962 molecules were subjected to XGraphBoost and 238 compounds were retained. The generated compounds all contained acrylamide group as warhead. In contrast to the screening of commercially available compounds, synthetic available score (SA score) calculated by RDKit was employed to filter out molecules that are difficult to synthesize and 105 compounds passed the filter. 115 compounds were retained and docked to the BTK protein to visualize the binding mode of the molecules by Glide in covalent docking mode. The workflow was shown in Fig. S3. Finally, four compounds were selected and subjected to biological evaluation.

Author contributions

Xiaojian Wang, Jing Jin, Jinping Hu and Xiaoguang Chen designed this project. Minjian Yang and Huimin Jiang assisted in designing this project. Minjian Yang and Zhuo Yang performed the chemical synthesis. Xue Liu and Hanyu Sun assisted in chemical synthesis. Huimin Jiang and Mengyao Hao performed in vitro assays of BTK. Minjian Yang, and Xiaojian Wang contributed to the writing, review and editing of the manuscript. All authors have given approval to the final version of the manuscript.

Declaration of competing interest

The authors declare that they have no known competing financial interests or personal relationships that could have appeared to influence the work reported in this paper.

Data availability

No data was used for the research described in the article.

Acknowledgments

This work was financially supported by CAMS Innovation Fund for Medical Sciences (CIFMS, no. 2021-I2M-1-028) and Disciplines Construction Project (Grant 201920200802). We thank Dr. Yadong Chen for the support of the docking studies.

Appendix A. Supplementary data

Supplementary data to this article can be found online at <https://doi.org/10.1016/j.ejmech.2022.114611>.

References

- [1] C. Brunner, B. Müller, T. Wirth, Bruton's tyrosine kinase is involved in innate and adaptive immunity, *Histol. Histopathol.* 20 (2005) 945–955. <http://hdl.handle.net/10201/22503>.
- [2] J.M. Bradshaw, The src, syk, and tec family kinases: distinct types of molecular switches, *Cell. Signal.* 22 (2010) 1175–1184, <https://doi.org/10.1016/j.cellsig.2010.03.001>.
- [3] A. Satterthwaite, Z. Li, O.N. Witte, Btk function in b cell development and response, *Semin. Immunol.* 10 (1998) 309–316, <https://doi.org/10.1006/smim.1998.0123>.
- [4] J.A. Di Paolo, T. Huang, M. Balazs, J. Barbosa, K.H. Barck, B.J. Bravo, R.A. Carano, J. Darow, D.R. Davies, L.E. DeForge, L. Diehl, R. Ferrando, S.L. Gallion, A. M. Giannetti, P. Grubing, V. Hurez, S.G. Hymowitz, R. Jones, J.E. Kropf, W.P. Lee, P.M. Maciejewski, S.A. Mitchell, H. Rong, B.L. Staker, J.A. Whitney, S. Yeh, W. B. Young, C. Yu, J. Zhang, K. Reif, K.S. Currie, Specific btk inhibition suppresses b cell- and myeloid cell-mediated arthritis, *Nat. Chem. Biol.* 7 (2011) 41–50, <https://doi.org/10.1038/nchembio.481>.
- [5] K.D. Puri, J.A. Di Paolo, M.R. Gold, B-cell receptor signaling inhibitors for treatment of autoimmune inflammatory diseases and b-cell malignancies, *Int. Rev. Immunol.* 32 (2013) 397–427, <https://doi.org/10.3109/08830185.2013.818140>.
- [6] J. Singh, The ascension of targeted covalent inhibitors, *J. Med. Chem.* 65 (2022) 5886–5901, <https://doi.org/10.1021/acs.jmedchem.1c02134>.
- [7] J.R. Brown, Ibrutinib (PCI-32765), the first btk (bruton's tyrosine kinase) inhibitor in clinical trials, *Curr. Hematol. Malig. Rep.* 8 (2013) 1–6, <https://doi.org/10.1007/s11899-012-0147-9>.

- [8] A. Aw, J.R. Brown, Current status of bruton's tyrosine kinase inhibitor development and use in b-cell malignancies, *Drugs Aging* 34 (2017) 509–527, <https://doi.org/10.1007/s40266-017-0468-4>.
- [9] Z. Zhao, P.E. Bourne, Progress with covalent small-molecule kinase inhibitors, *Drug Discov. Today* 23 (2018) 727–735, <https://doi.org/10.1016/j.drudis.2018.01.035>.
- [10] J. Wu, M. Zhang, D. Liu, Acalabrutinib (acp-196): a selective second-generation btk inhibitor, *J. Hematol. Oncol.* 9 (2016) 21, <https://doi.org/10.1186/s13045-016-0250-9>.
- [11] Y. Guo, Y. Liu, N. Hu, D. Yu, C. Zhou, G. Shi, B. Zhang, M. Wei, J. Liu, L. Luo, Z. Tang, H. Song, Y. Guo, X. Liu, D. Su, S. Zhang, X. Song, X. Zhou, Y. Hong, S. Chen, Z. Cheng, S. Young, Q. Wei, H. Wang, Q. Wang, L. Lv, F. Wang, H. Xu, H. Sun, H. Xing, N. Li, W. Zhang, Z. Wang, G. Liu, Z. Sun, D. Zhou, W. Li, L. Liu, L. Wang, Z. Wang, Discovery of zanubrutinib (bgb-3111), a novel, potent, and selective covalent inhibitor of bruton's tyrosine kinase, *J. Med. Chem.* 62 (2019) 7923–7940, <https://doi.org/10.1021/acs.jmedchem.9b00687>.
- [12] H.S. Walter, S.A. Rule, M.J. Dyer, L. Karlin, C. Jones, B. Cazin, P. Quittet, N. Shah, C.V. Hutchinson, H. Honda, K. Duffy, J. Birkett, V. Jamieson, N. Courtenay-Luck, T. Yoshizawa, J. Sharpe, T. Ohno, S. Abe, A. Nishimura, G. Cartron, F. Morschhauser, C. Fegan, G. Salles, A phase 1 clinical trial of the selective btk inhibitor onto/gs-4059 in relapsed and refractory mature b-cell malignancies, *Blood* 127 (2016) 411–419, <https://doi.org/10.1182/blood-2015-08-664086>.
- [13] S. Dhillon, Orelabrutinib: first approval, *Drugs* 81 (2021) 503–507, <https://doi.org/10.1007/s40265-021-01482-5>.
- [14] S.H. Watterson, G.V. De Luca, Q. Shi, C.M. Langevine, Q. Liu, D.G. Batt, M. Beaudoin Bertrand, H. Gong, J. Dai, S. Yip, P. Li, D. Sun, D.-R. Wu, C. Wang, Y. Zhang, S.C. Traeger, M.A. Pattoli, S. Skala, L. Cheng, M.T. Obermeier, R. Vickery, L.N. Disanza, C.J. D'Arienzo, Y. Zhang, E. Heimrich, K.M. Gillooly, T. L. Taylor, C. Pulicicchio, K.W. McIntyre, M.A. Galella, A.J. Tebben, J. K. Muckelbauer, C. Chang, R. Rampulla, A. Mathur, L. Salter-Cid, J.C. Barrish, P. H. Carter, A. Fura, J.R. Burke, J.A. Tino, Discovery of 6-fluoro-5-(r)-(3-(s)-(8-fluoro-1-methyl-2,4-dioxo-1,2-dihydroquinazolin-3(4h)-yl)-2-methylphenyl) -2-(s)-(2-hydroxypropan-2-yl)-2,3,4,9-tetrahydro-1h-carbazole-8-carboxamide (bms-986142): a reversible inhibitor of bruton's tyrosine kinase (btk) conformationally constrained by two locked atropisomers, *J. Med. Chem.* 59 (2016) 9173–9200, <https://doi.org/10.1021/acs.jmedchem.6b01088>.
- [15] J.J. Crawford, A.R. Johnson, D.L. Misner, L.D. Belmont, G. Castanedo, R. Choy, M. Coraggio, L. Dong, C. Eigenbrot, R. Erickson, N. Ghilardi, J. Hau, A. Katewa, P. B. Kohli, W. Lee, J.W. Lubach, B.S. McKenzie, D.F. Ortwine, L. Schutt, S. Tay, B. Wei, K. Reif, L. Liu, H. Wong, W.B. Young, Discovery of gcd-0853: a potent, selective, and noncovalent bruton's tyrosine kinase inhibitor in early clinical development, *J. Med. Chem.* 61 (2018) 2227–2245, <https://doi.org/10.1021/acs.jmedchem.7b01712>.
- [16] B. Ma, T. Bohnert, K.L. Otipoby, E. Tien, M. Arefayene, J. Bai, B. Bajrami, E. Bame, T.R. Chan, M. Humora, J.M. MacPhee, D. Marcotte, D. Mehta, C.M. Metrick, G. Moniz, E. Polack, U. Poreci, A. Prefontaine, S. Sheikh, P. Schroeder, K. Smirnakis, L. Zhang, F. Zheng, B.T. Hopkins, Discovery of biib068: a selective, potent, reversible bruton's tyrosine kinase inhibitor as an orally efficacious agent for autoimmune diseases, *J. Med. Chem.* 63 (2020) 12526–12541, <https://doi.org/10.1021/acs.jmedchem.0c00702>.
- [17] B.T. Hopkins, E. Bame, B. Bajrami, C. Black, T. Bohnert, C. Boiselle, D. Burdette, J. C. Burns, L. Delva, D. Donaldson, R. Grater, C. Gu, M. Hoemberger, J. Johnson,
- S. Kapadnis, K. King, M. Lulla, B. Ma, I. Marx, T. Magee, R. Meissner, C.M. Metrick, M. Mingueau, P. Murugan, K.L. Otipoby, E. Polack, U. Poreci, R. Prince, A. M. Roach, C. Rowbottom, J.C. Santoro, P. Schroeder, H. Tang, E. Tien, F. Zhang, J. Lyssikatos, Discovery and preclinical characterization of biib091, a reversible, selective btk inhibitor for the treatment of multiple sclerosis, *J. Med. Chem.* (2021), <https://doi.org/10.1021/acs.jmedchem.1c00926>.
- [18] W. Kawahata, T. Asami, T. Kiyoi, T. Irie, S. Kashimoto, H. Furuchi, M. Sawa, Discovery of as-1763: a potent, selective, noncovalent, and orally available inhibitor of bruton's tyrosine kinase, *J. Med. Chem.* 64 (2021) 14129–14141, <https://doi.org/10.1021/acs.jmedchem.1c01279>.
- [19] A.P. Bye, A.J. Unsworth, M.J. Desborough, C.A.T. Hildyard, N. Appleby, D. Bruce, N. Krieg, S.H. Nock, T. Sage, C.E. Hughes, J.M. Gibbins, Severe platelet dysfunction in nhl patients receiving ibrutinib is absent in patients receiving acalabrutinib, *Blood Adv* 1 (2017) 2610–2623, <https://doi.org/10.1182/bloodadvances.2017011999>.
- [20] Y.A. Senis, A. Mazharian, J. Mori, Src family kinases: at the forefront of platelet activation, *Blood* 124 (2014) 2013–2024, <https://doi.org/10.1182/blood-2014-01-453134>.
- [21] R. de Vries, J.W. Smit, P. Hellemans, J. Jiao, J. Murphy, D. Skee, J. Snoeys, J. Stukbuntherng, M. Vliegen, L. de Zwart, E. Mannaert, J. de Jong, Stable isotope-labelled intravenous microdose for absolute bioavailability and effect of grapefruit juice on ibrutinib in healthy adults, *Br. J. Clin. Pharmacol.* 81 (2016) 235–245, <https://doi.org/10.1111/bcp.12787>.
- [22] D. Deng, X. Chen, R. Zhang, Z. Lei, X. Wang, F. Zhou, Xgraphboost, Extracting graph neural network-based features for a better prediction of molecular properties, *J. Chem. Inf. Model.* (2021) 2697–2705, <https://doi.org/10.1021/acs.jcim.0c01489>.
- [23] R. Pulz, D. Angst, J. Dawson, F. Gessier, S. Gutmann, R. Hersperger, A. Hinniger, P. Janser, G. Koch, L. Revesz, A. Vulpetti, R. Waelchli, A. Zimmerlin, B. Cenni, Design of potent and selective covalent inhibitors of bruton's tyrosine kinase targeting an inactive conformation, *ACS Med. Chem. Lett.* 10 (2019) 1467–1472, <https://doi.org/10.1021/acsmedchemlett.9b00317>.
- [24] R.D. Caldwell, H. Qiu, B.C. Askew, A.T. Bender, N. Brugger, M. Camps, M. Dhanabal, V. Dutt, T. Eichhorn, A.S. Gardberg, A. Goutopoulos, R. Grenningloh, J. Head, B. Healey, B.L. Hodous, B.R. Huck, T.L. Johnson, C. Jones, R.C. Jones, I. Mochalkin, F. Morandi, N. Nguyen, M. Meyring, J.R. Potnick, D.C. Santos, R. Schmidt, B. Sherer, A. Shutes, K. Urbahns, A.V. Follis, A.A. Wegener, S. C. Zimmerli, L. Liu-Bujalski, Discovery of evobrutinib: an oral, potent, and highly selective, covalent bruton's tyrosine kinase (btk) inhibitor for the treatment of immunological diseases, *J. Med. Chem.* 62 (2019) 7643–7655, <https://doi.org/10.1021/acs.jmedchem.9b00794>.
- [25] T. Li, R. Perez-Soler, Skin toxicities associated with epidermal growth factor receptor inhibitors, *Target. Oncol.* 4 (2009) 107–119, <https://doi.org/10.1007/s11523-009-0114-0>.
- [26] B. Melosky, Supportive care treatments for toxicities of anti-egfr and other targeted agents, *Curr. Oncol.* 19 (2012) S59–S63, <https://doi.org/10.3747/co.19.1054>.
- [27] J.B. Baell, G.A. Holloway, New substructure filters for removal of pan assay interference compounds (pains) from screening libraries and for their exclusion in bioassays, *J. Med. Chem.* 53 (2010) 2719–2740, <https://doi.org/10.1021/jm901137j>.